Article

Immunity

Febrile Temperature Critically Controls the Differentiation and Pathogenicity of T Helper 17 Cells

Graphical Abstract

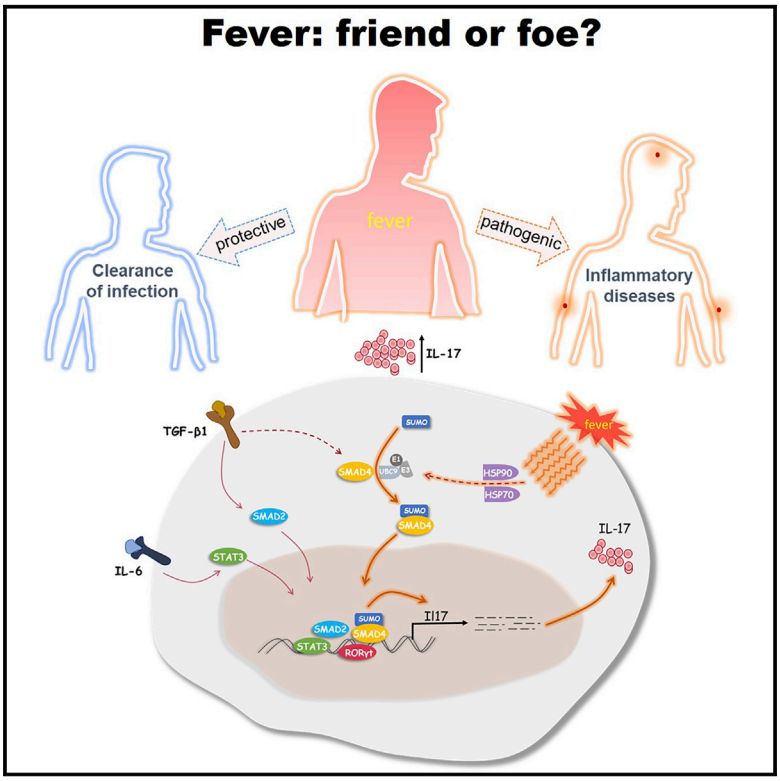

Authors

Xiaohu Wang, Lu Ni, Siyuan Wan, Xiaohong Zhao, Xiao Ding, Anne Dejean, Chen Dong

Correspondence

wangxhu@tsinghua.edu.cn (X.W.), chendong@tsinghua.edu.cn (C.D.)

In Brief

Fever has been proposed to have an evolutionarily conserved protective role in infectious diseases. In this study, Wang et al. demonstrate a selective role of fever in boosting Th17 cell differentiation and associated pathogenic functions in autoimmune diseases via heat-shock-response-induced SMAD4 SUMOylation.

Highlights

- Treatment with anti-pyretic regents reduced Th17 cell differentiation *in vivo*
- Febrile temperature promotes the differentiation and pathogenicity of Th17 cells
- SMAD4 SUMOylation is indispensable for Th17 cell differentiation at febrile temperature
- Smad4-deficient mice are resistant to experimental autoimmune encephalomyelitis (EAE)

Wang et al., 2020, Immunity *52*, 1–14
February 18, 2020 © 2020 Published by Elsevier Inc.
https://doi.org/10.1016/j.immuni.2020.01.006

CellPress

Please cite this article in press as: Wang et al., Febrile Temperature Critically Controls the Differentiation and Pathogenicity of T Helper 17 Cells, Immunity (2020), https://doi.org/10.1016/j.immuni.2020.01.006

CellPress

Febrile Temperature Critically Controls the Differentiation and Pathogenicity of T Helper 17 Cells

Xiaohu Wang,[1,4,*] Lu Ni,[1,4] Siyuan Wan,[1] Xiaohong Zhao,[1] Xiao Ding,[1] Anne Dejean,[2] and Chen Dong[1,3,5,*]
[1]Institute of Immunology and School of Medicine, Tsinghua University, Beijing 100084, China
[2]Nuclear Organization and Oncogenesis Laboratory, Department of Cell Biology and Infection, INSERM U993, Institute Pasteur, Paris 75015, France
[3]Beijing Key Lab for Immunological Research on Chronic Diseases, Beijing 100084, China
[4]These authors contributed equally
[5]Lead Contact
*Correspondence: wangxhu@tsinghua.edu.cn (X.W.), chendong@tsinghua.edu.cn (C.D.)
https://doi.org/10.1016/j.immuni.2020.01.006

SUMMARY

Fever, an evolutionarily conserved physiological response to infection, is also commonly associated with many autoimmune diseases, but its role in T cell differentiation and autoimmunity remains largely unclear. T helper 17 (Th17) cells are critical in host defense and autoinflammatory diseases, with distinct phenotypes and pathogenicity. Here, we show that febrile temperature selectively regulated Th17 cell differentiation *in vitro* in enhancing interleukin-17 (IL-17), IL-17F, and IL-22 expression. Th17 cells generated under febrile temperature (38.5°C–39.5°C), compared with those under 37°C, showed enhanced pathogenic gene expression with increased pro-inflammatory activities *in vivo*. Mechanistically, febrile temperature promoted SUMOylation of SMAD4 transcription factor to facilitate its nuclear localization; SMAD4 deficiency selectively abrogated the effects of febrile temperature on Th17 cell differentiation both *in vitro* and ameliorated an autoimmune disease model. Our results thus demonstrate a critical role of fever in shaping adaptive immune responses with implications in autoimmune diseases.

INTRODUCTION

Fever—a physiological response commonly associated with infections, injuries, and neoplasia (Pasikhova et al., 2017)—is evolutionarily conserved in both endothermic and ectothermic animals. Febrile-range temperatures (1°C–4°C above basal core body temperature) are suggested to have a survival advantage in infectious diseases, possibly through inhibiting pathogen growth and boosting protective immune responses (Evans et al., 2015; Hasday et al., 2014; Lin et al., 2019). A key role of fever in the immune system is to stimulate the innate immune system, such as release of neutrophils in periphery, production of cytokines and nitric oxide from macrophages or dendritic cells, promotion of leukocyte trafficking, and enhancement of their phagocytic, bacteriolytic, cytolytic or antigen presentation functions (Evans et al., 2015; Hasday et al., 2014). Fever is also a shared clinical symptom in many autoimmune diseases, including rheumatoid arthritis, systemic lupus erythematosus, adult-onset Still's disease, rheumatic fever, and inflammatory bowel disease (Limper et al., 2010; Shang et al., 2017). Fever can be observed at both early and active stages of autoimmune diseases, and ~20% of patients with clinical fever of unknown origins are diagnosed later with autoimmune diseases (Limper et al., 2010; Shang et al., 2017), suggesting a possible pathogenic role of fever in autoimmune diseases.

T helper 17 (Th17) cells play an important protective role in host defense against fungal and extracellular bacterial infections, as well as in mucosal barrier maintenance (Eming et al., 2017; Stockinger and Omenetti, 2017). However, excessive Th17 cell responses cause chronic tissue inflammation associated with human autoimmune diseases (Stockinger and Omenetti, 2017). The differentiation of Th17 cells is initiated by interleukin-6 (IL-6) and transforming growth factor-β (TGF-β). IL-6 acts mainly through activating the STAT3 transcription factor (Yang et al., 2007). Downstream signaling of TGF-β involved in Th17 cell differentiation has also been studied. Canonically, TGF-β activates SMAD2 and SMAD3, which form a heterotrimeric complex with SMAD4 and translocate into nucleus to mediate downstream gene expression. SMAD2 is required for Th17 cell differentiation (Malhotra et al., 2010; Martinez et al., 2010), while SMAD3 may play a negative role (Martinez et al., 2009) but also compensate for SMAD2 deficiency (Zhang, 2018). Our earlier report demonstrated a dispensable role of SMAD4 for Th17 cell differentiation *in vitro* (Yang et al., 2008), which was supported by several subsequent studies (Hahn et al., 2011; Zhang et al., 2017). However, a recent publication reported a negative role of SMAD4 in suppressing IL-17 expression when T cells were cultured under IL-6-only conditions via recruiting the transcription repressor SKI (Zhang et al., 2017). In contrast, under complete Th17 cell-polarizing conditions, TGF-β causes degradation of SKI to release the inhibitory effect of SMAD4 (Zhang et al., 2017), and together with IL-6, induce robust expression of RORγt—the lineage-specific

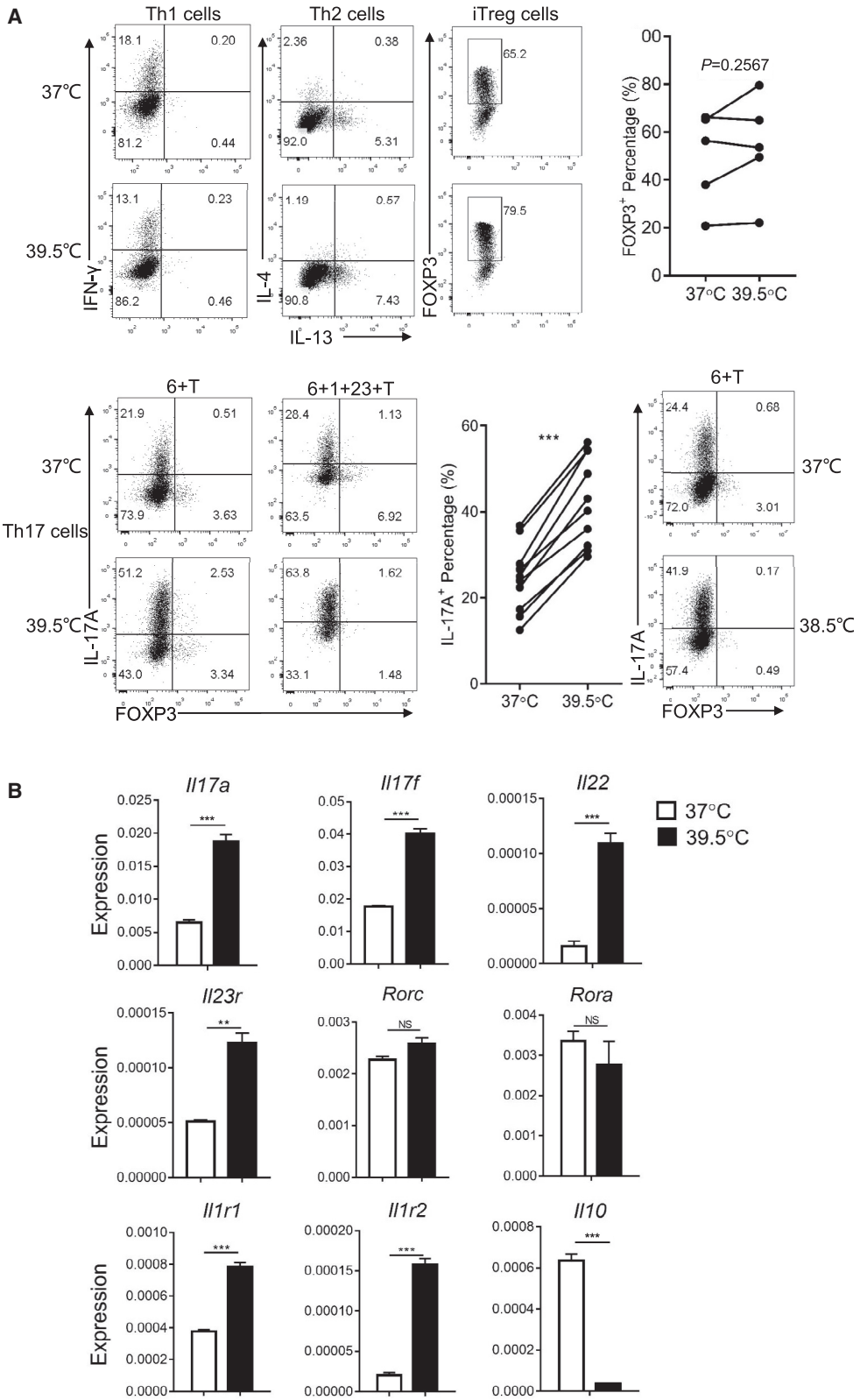

(legend on next page)

transcriptional factor directly controlling production of IL-17 and IL-17F (Stockinger and Omenetti, 2017), the major effect cytokines in Th17 cells.

Under *in vivo* settings, there is growing evidence that Th17 cells generated in the mucosal tissue, associated with hemostatic barrier regulatory function, are phenotypically distinct from those in the inflamed tissues of autoimmune diseases (Esplugues et al., 2011; Gaublomme et al., 2015), and their pathogenicity could be affected by surrounding microenvironments, including cytokines TGF-β3, IL-1β, and IL-23, salt, and microbiota (Kleinewietfeld et al., 2013; Lee et al., 2012; Stockinger and Omenetti, 2017; Wu et al., 2013).

Non-steroid anti-inflammation drugs generally featured with anti-pyretic properties, including aspirin and rofecoxib, not only reduce inflammation in human patients (Li et al., 2017) but also effectively alleviate the experimental autoimmune encephalomyelitis (EAE) model (Mondal et al., 2018; Ni et al., 2007). In this study, we examined the role of fever in adaptive immunity and found that febrile temperature selectively enhanced Th17 cell differentiation and pro-inflammatory function *in vitro*. Mechanistically, febrile temperature enhanced global amounts of protein SUMOylations, a common response to various stress stimuli (Saitoh and Hinchey, 2000). Of note, SMAD4, though not required for Th17 cell differentiation under normal temperature, was selectively required for febrile-temperature-dependent Th17 cell differentiation *in vitro* and *in vivo*, through SUMOylation at its K113 and K159 residues. Therefore, our studies demonstrate a pathogenic mechanism whereby fever promotes autoimmune diseases through regulating the differentiation and pathogenicity of Th17 cells.

RESULTS

Febrile Temperature Selectively Promotes Th17 Cell Differentiation *In Vitro* via Heat Shock Responses

To understand the role of fever in T cell response and related autoimmunity, naive $CD4^+$ T cells were cultured *in vitro* under Th1, Th2, Th17, and T regulatory (Treg) cell-polarizing conditions at 37°C or 39.5°C for 3–4 days. Febrile temperature did not affect Th1, Th2, or induced (iTreg) cell differentiation but selectively and robustly enhanced Th17 cell differentiation as determined by intracellular staining of IL-17A (~2-fold increase) under both sub-optimal (IL-6+TGF-β1) and optimal conditions (IL-6+TGF-β1+IL-1β+IL-23) (Figure 1A). It is noticed that a mild temperature increase (38.5°C) caused a similar degree of enhancement of Th17 cell differentiation, further confirming that Th17 cell differentiation is temperature sensitive (Figure 1A). At the mRNA level, febrile temperature significantly enhanced the expression of key Th17 cell cytokine genes, including *Il17a*, *Il17f*, and *Il22*, as well as cytokine receptor genes *Il1r1* and *Il1r2*, but greatly reduced the expression of anti-inflammatory cytokine *Il10* (Figures 1A and 1B). However, the mRNA amounts for *Rorc* and *Rora* were not significantly affected (Figure 1B).

Heat shock responses are characterized by activation and induction of heat shock factors and heat shock proteins (Singh and Hasday, 2013). Consistently, expression of heat shock proteins, including *Hsp40*, *Hsp60*, *Hsp70*, *Hsp90*, and *Hsp110 h*, and the master heat shock factors HSF1 and HSF2 were rapidly induced in Th17 cells cultured at 39.5°C at mRNA or protein levels, respectively (Figures S1A and S1B). Heat shock protein inhibitors, such as NMS-E973 for HSP90 or VER155008 for HSP70, inhibited febrile-temperature-enhanced Th17 cell differentiation (Figure S1C). Additionally, short hairpin RNA (shRNA) silencing *Hsp70* mRNA expression abolished febrile-temperature-associated Th17 cell differentiation, though its overexpression had no effect on Th17 cell induction at normal or febrile temperatures (Figures S1D and S1E), suggesting that *Hsp70* upregulation is necessary but not sufficient to potentiate Th17 cell differentiation at febrile temperatures. In multiple experiments, treatment with an HSP70 inhibitor slightly but consistently reduced Th17 cell differentiation under 37°C, suggesting a possible minor role for HSP-dependent stress response in normal Th17 cell differentiation.

Febrile Temperature Regulates Th17 Cell Differentiation *In Vivo*

The above studies support a selective role of febrile temperature in regulating Th17 cell differentiation *in vitro*. To investigate the role of febrile temperature *in vivo*, we first immunized C57BL/6 mice with MOG_{35-55} peptide emulsified in either complete Freund's adjuvant (CFA) at one dorsal side near the tail base by subcutaneous injection, and then monitored temperature changes at both involved (draining lymph nodes) and uninvolved inguinal lymph nodes with an infrared thermometer for 60 h; the anal temperature (indicating systemic body temperature) was also monitored using a digital thermometer. In the immunized mice, the draining lymph nodes showed increased peak temperature at 12 h, whereas the body temperature peaked around 24 h post-immunization, indicating a systemic fever response (Figure S2A).

To investigate the *in vivo* effect of fever, naive OT-II T cells were adoptively transferred into $Tcrbd^{-/-}$ mice, followed by OVA+CFA immunization. As expected, fever was readily induced as in the wild-type (WT) C57BL/6 mice post-immunization (Figures S2A and S2B) and was associated with increased expression of heat-shock-response-related genes in the donor OT-II

Figure 1. Febrile Temperature Enhanced Th17 Cell Differentiation

Naive $CD4^+$ T cells were polarized under Th1 (IFN-γ+IL-12+anti-IL-4+IL-2), Th2 (IL-4+anti-IFN-γ+IL-2), Th17 (IL-6+TGF-β1 or IL-6+IL-1β+IL-23+TGF-β1), or iTreg (TGF-β1+IL-2) culture condition for 3–4 days at 37°C or 39.5°C, respectively, and the cells were re-stimulated with phorbol-12-myristate-13-acetate, ionomycin, and Golgi stop for intracellular staining or with αCD3 for mRNA expression analysis.

(A) Top left: intracellular staining of lineage-specific cytokines or transcriptional factors in Th1, Th2, and iTreg cells. Top right: statistic data of iTreg cells polarized under 37°C or 39.5°C (n = 4). Bottom: intracellular staining of IL-17 and FOXP3 in Th17 cells polarized under 37°C, 39.5°C, or 38.5°C. Bottom middle: statistic data of the left febrile Th17 cell staining data.

(B) Real-time PCR data of mRNA expression in Th17 cells after 3 days' culture under 37°C or 39.5°C. The statistics were performed by Student's t test. *$p < 0.05$; **$p < 0.01$; ***$p < 0.001$. The data for T cell differentiation and real-time PCR were repeated at least 3 times with consistent results.

See also Figure S1.

cells, including *Hsf1*, *Hsf2*, *Hsp60*, *Hsp90*, and *Hsp110* (Figure 2A) as well as IL-17 expression (Figure 2B). Treatment with anti-pyretic drugs, such as aspirin or ibuprofen, not only reduced fever and fever-related gene expression (Figure 2A) but also decreased Th17 cell differentiation in the recipient mice (Figure 2B). These data strongly suggest a T cell-intrinsic effect of fever in regulating *in vivo* Th17 cell differentiation.

Febrile Temperature Increases the Pathogenicity of Th17 Cells

To further understand the effect of febrile temperature, an RNA sequencing (RNA-seq) assay was performed with Th17 cells generated at both 37°C and 39.5°C. Overall, 1,083 genes were upregulated in Th17 cells generated at 39.5°C ($p < 0.01$, fold change ≥ 1.5), compared with those at 37°C (Figure 3A). Pathway analysis revealed that the top listed pathways included genes involved in cytokine-cytokine receptor interaction and Th17 cell differentiation, such as *Il17*, *Il17f*, and *Il22* as well as *Il1r1*, *Il1r2*, and *Il23r*, which are critical for Th17 cell differentiation or effect function (Stockinger and Omenetti, 2017) (Figures 3A and S3A). Moreover, Th1-related transcription factors *Tbx21* and *Stat4*, necessary for Th17 cell-mediated autoimmune diseases (Bettelli et al., 2004; Chitnis et al., 2001), were also upregulated by febrile temperature (Figure 3A). In addition, differentiation at 39.5°C led to upregulation of transcription factors *Nr4a2* and *Nfatc1*, both of which directly regulate IL-17 expression and are important in EAE induction (Doi et al., 2008; Reppert et al., 2015; Zhu et al., 2017), as well as *Cd24a*, a positive regulator for Th17 cells and related autoimmunity (Bai et al., 2000; Zhu et al., 2017) (Figure 3A).

Febrile temperature also repressed 392 genes in Th17 cells (Figure 3A), enriched mostly with biosynthetic and metabolic pathways, including in fatty acids, sugar, and carbon backbone metabolism or biosynthesis, possibly because of heat-induced stress response (Figure S3A). The most highly repressed genes included *Gpr83*, encoding a Treg cell surface marker involved in suppressive activity (Hansen et al., 2006; Sugimoto et al., 2006), and *Cd62l* (sell), a naive T cell marker for T cell homing to peripheral lymphoid tissues (Wedepohl et al., 2012) (Figure 3A).

Th17 cells induced by IL-6+TGF-β1 are relatively non-pathogenic, and those generated in the presence of IL-23 or IL-6 in combination with TGF-β3 or IL-1 and IL-23 are more pathogenic (Ghoreschi et al., 2010; Lee et al., 2012). Among the 99 genes upregulated over 1.5-fold in pathogenic (TGF-β3+IL-6) versus non-pathogenic (TGF-β1+IL-6) Th17 cells (Lee et al., 2012), 30 of them were upregulated in Th17 cells induced at febrile temperatures (Figure 3B), including 22 genes also upregulated in Th17 cells induced by IL-1β, IL-6+IL-23 (Lee et al., 2012), including *Ccl3*, *Cxcl3*, *Tnfsf11*, *Tbx21*, and *Stat4* (Figure 3B). Gene set enrichment analysis (GSEA) showed that Th17 cells cultured at febrile temperature were more similar to the ones induced by IL-6, IL-1, and IL-23 than those induced by IL-6+TGF-β1 (Ghoreschi et al., 2010) (Figure 3C). In addition, they also exhibited gene expression patterns strongly correlated with those in pathogenic Th17 cells derived from inflamed CNS in EAE but not with those from non-pathogenic, gut-associated Th17 cells (Gaublomme et al., 2015) (Figure 3C). These data together indicate that Th17 cells generated under febrile temperature exhibit a strong correlation with pathogenic Th17 cells in the literatures, supporting the idea that Th17 cells generated *in vivo* may be under the influence of febrile temperature in the draining lymph nodes.

To validate the above findings, an acute lung inflammation model was performed in CD45.1 mice by adoptive transfer of CD45.2 OT-II Th17 cells that were induced by OVA-peptide and antigen-presenting cells (APCs) *in vitro* at 37°C or 39.5°C. Following intranasal administration of OVA protein, as expected, Th17 cells generated with febrile temperature induced significantly increased neutrophil infiltration in both the lung tissue and bronchoalveolar lavage fluid (BALF) than those generated at 37°C (Figures 3D and S3B), supporting a highly pro-inflammatory feature of Th17 cells induced at febrile temperatures.

Febrile Temperature Promotes Th17 Cell Differentiation through Enhancing SMAD4 SUMOylation and Its Nuclear Localization

To understand the mechanism underneath febrile Th17 cell differentiation, we first focused on STAT3 and SMAD2 and SMAD3, critical downstream transcription mediators of IL-6 and TGF-β signaling, respectively. However, febrile temperature did not affect their phosphorylation activation status (Figure S4A) and could still upregulate IL-17 expression in SMAD2-deficient T cells, though both IL-6 and TGF-β were indispensable for Th17 cell differentiation (Figures S4B and S4C), suggesting alternative mechanism(s) involved.

A recent study reported that SMAD4-deficient T cells can differentiate into Th17 cells under IL-6-only culture condition (Zhang et al., 2017), we therefore tested if febrile temperature could further increase IL-6-induced yet SMAD4-independent Th17 cell program. Consistent with previous findings (Hahn et al., 2011; Yang et al., 2008; Zhang et al., 2017), SMAD4-deficiency did not affect Th17 cell differentiation induced with complete Th17-polarizing cytokine cocktails (IL-6+TGF-β1 or IL-6+IL-1β+IL-23+TGF-β1) under normal 37°C culture condition but resulted in increased Th17 cell differentiation when cultured with cytokine cocktails containing IL-6 but lacking TGF-β1 signaling (IL-6+anti-TGF-β1 or IL-6+IL-1β+IL-23+anti-TGF-β1), in which anti-TGF-β1 was used to neutralize endogenous TGF-β1 in the culture (Figure 4A). Under 39.5°C, *Smad4*$^{\Delta CD4}$ T cells failed in upregulating IL-17 expression under both IL-6-only and complete Th17-polarizing culture conditions (Figure 4A), suggesting a necessary positive role of SMAD4 in controlling Th17 cell differentiation at febrile temperatures.

The nuclear localization and transcription activity of SMAD4 is regulated by SUMOylation at its K113 and K159 residues (Lin et al., 2003), and an important consequence of heat shock response is the rapid increase of cellular amounts of protein SUMOylations (Gareau and Lima, 2010). These previous findings prompted us to speculate a role of SUMOylation pathway in Th17 cell differentiation at febrile temperatures. We therefore collected T cells activated and cultured under Th17-polarizing conditions for 24 h at 37°C or 39.5°C and then analyzed cellular proteins conjugated to SUMO2, a key SUMO moiety in the SUMOylation pathway. As expected, febrile temperature increased total cellular amounts of SUMOylated proteins in Th17 cells, as determined by increase in SUMO2-containing high-molecular-weight proteins (Figure 4B). Consistently, the amount of SUMOylated

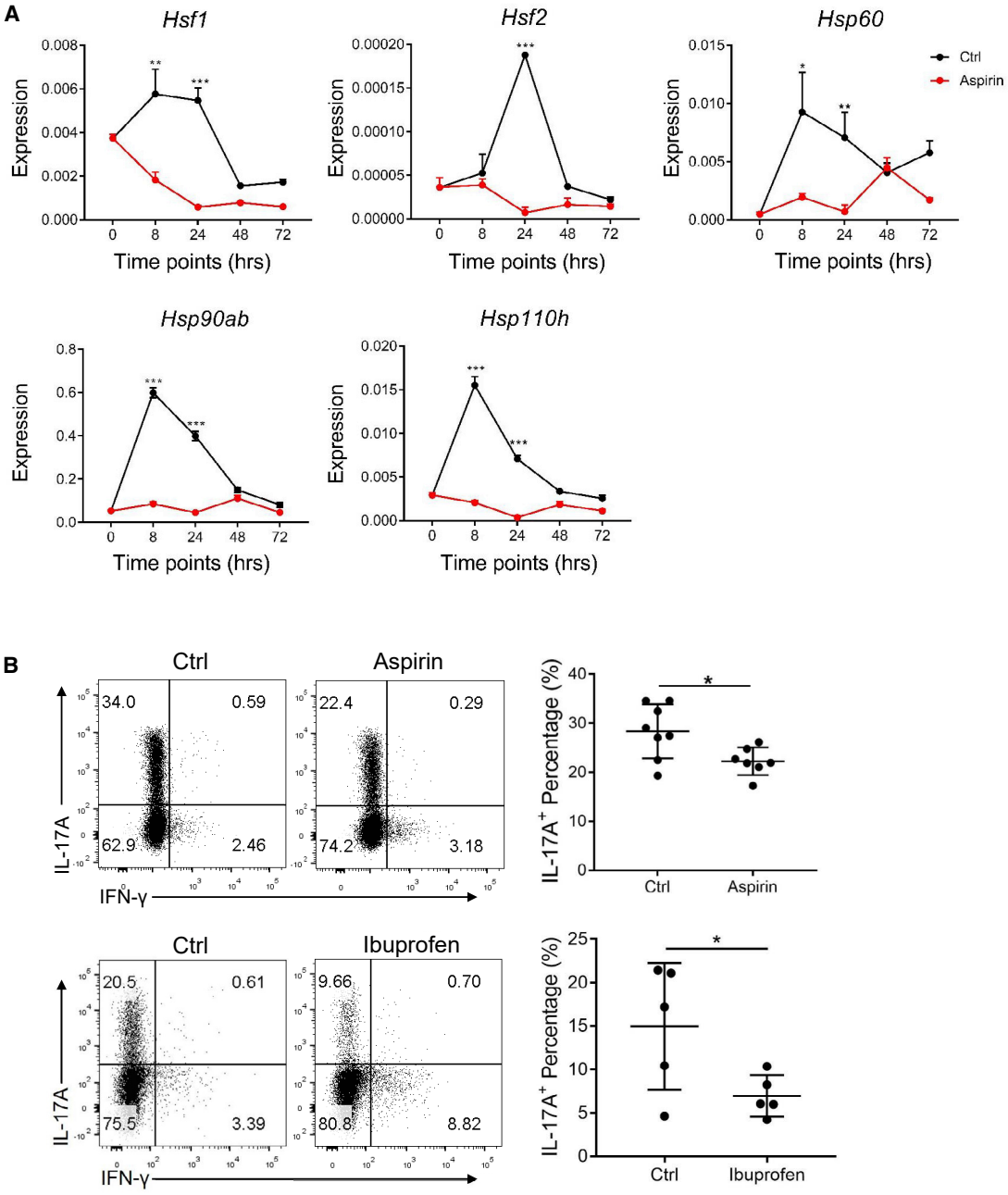

Figure 2. Anti-pyretic Drugs Reduced Heat Shock Response and Th17 Cell Differentiation *In Vivo*

Naive OT-II cells were intravenously transferred into *Tcrbd*$^{-/-}$ mice (~2×10^5 cells/mouse), followed by OVA+CFA immunization. The mice were treated by oral gavage with aspirin (2 mg/kg body weight, dissolved in 0.5% methyl cellulose solution, n = 7) and control solution (n = 7) twice a day or ibuprofen (50 mg/kg body weight, dissolved in 0.5% methyl cellulose, n = 5) and control (n = 5) daily throughout the experiment. The transferred OT-II T cells ($CD4^+CD3^+$) were isolated from the draining lymph nodes at different time points as indicated and analyzed for heat-shock-related gene expression.

(A) Relative mRNA expression of *Hsf1*, *Hsf2*, *Hsp60*, *Hsp90*, and *Hsp110 h* (for each time point, 2–3 mice were sacrificed, and the OT-II cells were isolated and pooled together for real-time PCR analysis; the results shown here represent one of the three independent results).

(B) Left: intracellular staining of IL-17 and IFN-γ in the donor OT-II T cells after aspirin or ibuprofen treatment for 7 days. Right: statistic data of IL-17A expression in the donor OT-II T cells after aspirin or ibuprofen treatment. The ibuprofen- or aspirin-treatment experiments were repeated 2 or 3 times with consistent results, respectively. The statistics were performed by Student's t test. *$p < 0.05$; **$p < 0.01$; ***$p < 0.001$.

See also Figure S2.

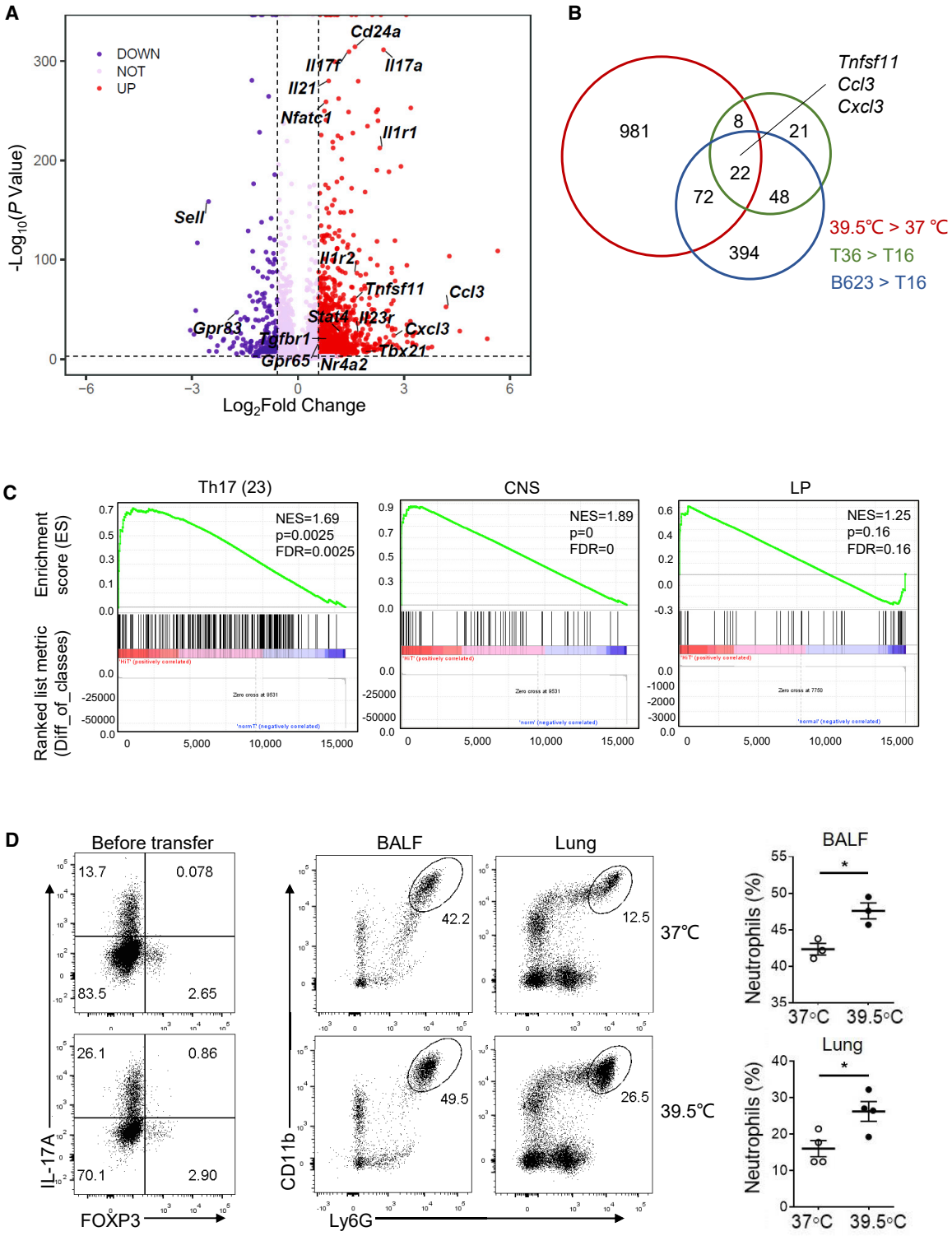

Figure 3. Febrile-Temperature-Induced Pathogenic Th17 Cell Program

Th17 cells induced at 37°C or 39.5°C with IL-6 and TGF-β1 were collected and used for whole-genome transcriptome analysis.

(A) Volcano plots of differential gene expression pattern between Th17 cells induced at 39.5°C and 37°C.

(B) Overlap of febrile temperature upregulated genes (≥1.5-fold increase) with those upregulated by TGF-β3+IL-6 (T36) or IL-1β+IL-6+IL-23 (B623) versus TGF-β1+IL-6 (T16).

(C) GSEA analysis of RNA-seq data obtained from febrile Th17 cells versus IL-23-induced Th17 cells, referred to as Th17 (23), or Th17 cells derived in the CNS of the EAE model or homeostatic lamina propia tissues (LP).

(legend continued on next page)

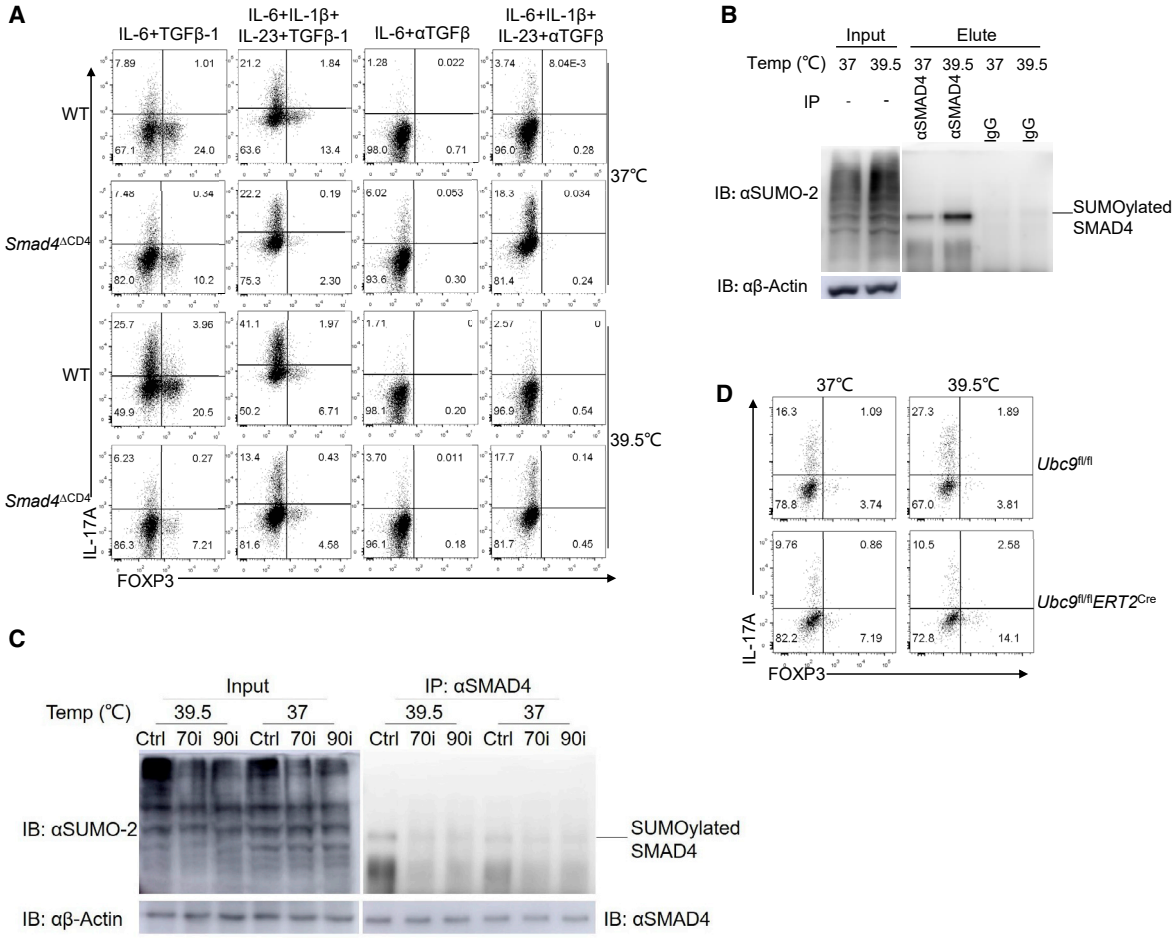

Figure 4. Febrile Th17 Cell Differentiation Was Dependent on SMAD4 SUMOylation.

(A) WT (*Smad4*$^{fl/fl}$) and *Smad4*$^{-/-}$ (*Smad4*$^{fl/fl}$*CD4*^{Cre}) naive T cells were polarized with complete Th17-polarizing conditions (IL-6+TGF-β1 or IL-6+IL-1β+IL-23+TGF-β1) or IL-6 culture conditions (IL-6+anti-TGF-β or IL-6+IL-1β+IL-23+anti-TGF-β) at 37°C or 39.5°C and analyzed by flow cytometry. The results shown here represent one of the two independent experiments.

(B) Immuno-blot of total cellular SUMO2-conjugated proteins and SUMOylated SMAD4 (immunoprecipitated with αSMAD4 and then blotted by αSUMO2) in Th17 cells induced at 37°C and 39.5°C for 24 h in the presence of IL-6 and TGF-β1. β-Actin was blotted as a loading control. The results shown here represent one of the two independent experiments.

(C) Immuno blot of total cellular SUMO2-conjugated proteins and SUMOylated SMAD4 (immunoprecipitated with αSMAD4 and then blotted by αSUMO2) in T cells polarized under Th17 cell condition (IL-6+TGF-β1) cultured with or without HSP70 inhibitor (10 μM) or HSP90 inhibitor (0.2 μM) at 37°C and 39.5°C for 24 h. β-actin was also blotted as control. The results shown here represent one of the two independent experiments.

(D) Intracellular staining of IL-17A and FOXP3 in WT (*Ubc9*$^{fl/fl}$) and Ubc9-deficient (*Ubc9*$^{fl/fl}$ERT2^{Cre}) Th17 cells induced with IL-6 and TGF-β1 at 37°C and 39.5°C in the presence of tamoxifen. The results shown here represent one of two independent experiments.

Please also see Figure S4.

SMAD4 was also increased at 24 h (Figure 4B), which was detected as early as 4 h post-febrile-temperature treatment (Figure S4D), indicating a direct role of heat-induced stress response in promoting SMAD4 SUMOylation. To further confirm this, T cells were polarized under Th17 cell culture condition (IL-6+TGF-β1) in the presence of HSP70 and HSP90 inhibitors. These inhibitors reduced global cellular amounts of SUMOylated proteins, including SUMOylated SMAD4 (Figure 4C), and also abrogated increased IL-17 expression at 39.5°C (Figure S1C), suggesting a functional role of heat shock response in regulating SMAD4 SUMOylation and Th17 cell differentiation.

To confirm the functional of SUMOylation in Th17 cell differentiation, UBC9, the only E2-conjugating enzyme in the SUMOylation pathway (Gareau and Lima, 2010), was selectively

(D) Left: intracellular-staining data of Th17 cells induced using the APCs-OT-II co-culture system at 37°C and 39.5°C, respectively. Middle: intracellular staining data of neutrophils (CD11b^{+}Ly6G^{+}) infiltrated in the BALF and lung tissue. Right: statistic data of the percentage of infiltrated neutrophils (the results shown here represent one of two independent results).The statistics were performed by Student's t test. *$p < 0.05$; **$p < 0.01$; ***$p < 0.001$.

See also Figure S3.

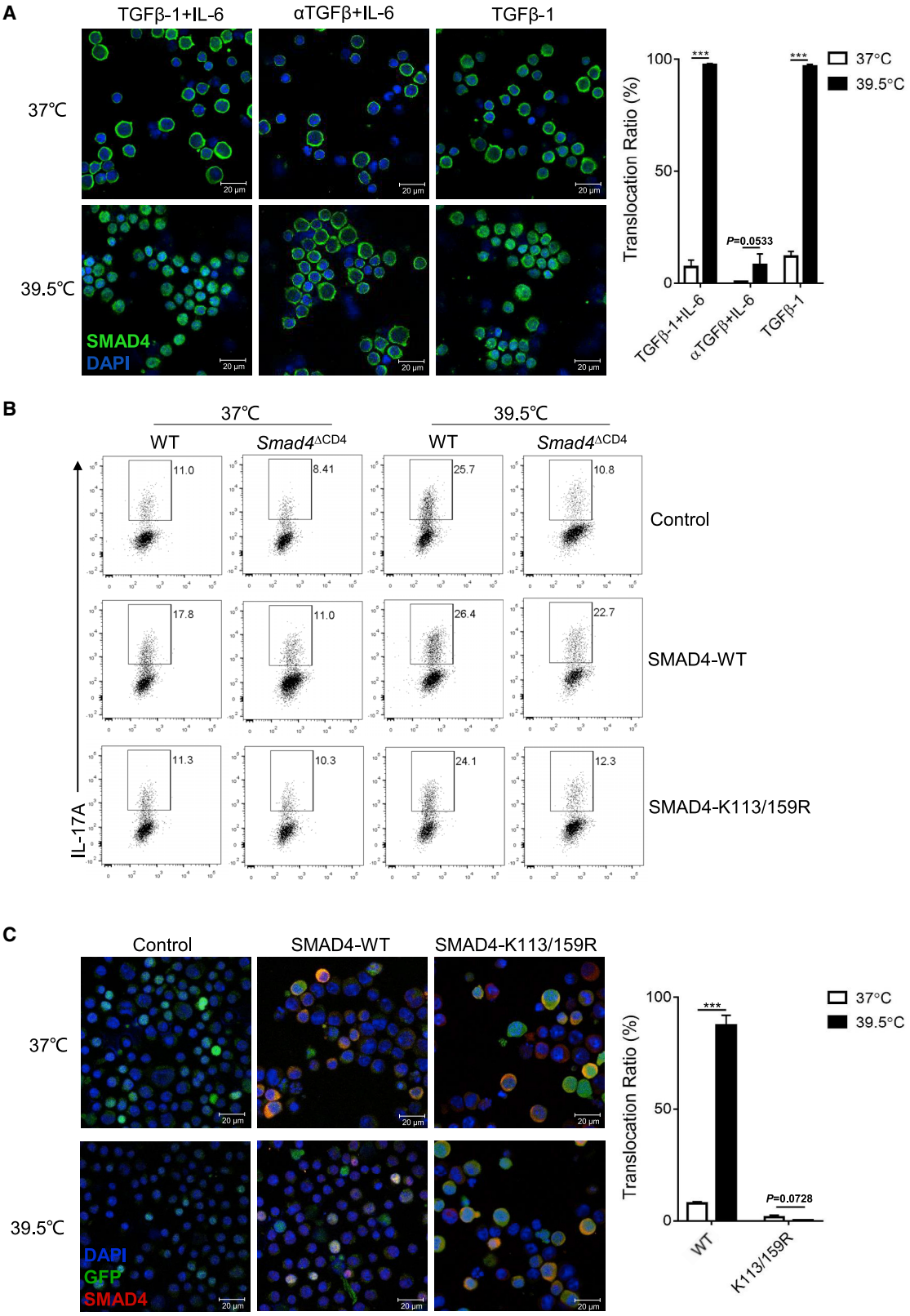

(legend on next page)

ablated in activated T cells using the CreERT2-mediated inducible deletion strategy. As expected, UBC9 deficiency completely abolished the effect by febrile temperature on Th17 cell differentiation (Figure 4D), suggesting an essential role of SUMOylation for febrile Th17 cell differentiation. It is noticed that UBC9 deficiency also reduced IL-17 expression at 37°C, suggesting a role for SUMOylation in Th17 cells at normal physiological temperature, likely in a SMAD4-independent manner (Figure 4D).

To investigate whether SMAD4 SUMOylation indeed regulates Th17 cell differentiation at febrile temperatures, we first examined the subcellular localization of SMAD4 by immunofluorescence microscopy, and it was found mostly localized in the nuclei of Th17 cells 24 h post-culture at 39.5°C but barely at 37°C (Figure 5A). This phenomenon was dependent on TGF-β because IL-6 alone could not cause SMAD4 nuclear localization, whereas TGF-β-only culture condition was sufficient to induce SMAD4 nuclear localization at elevated temperature (Figure 5A). In addition, when we overexpressed WT SMAD4 or the SMAD4- K113R/K159R double mutant in *Smad4*$^{-/-}$ T cells (infected cells carry GFP reporter signal derived from the retroviral plasmid). WT, but not mutant, *Smad4* restored T cell responsiveness to febrile temperature in IL-17 expression in *Smad4*$^{-/-}$ T cells (Figure 5B). As expected, the mutant SMAD4 protein did not respond to the febrile temperature in their nuclear localization (Figure 5C).

SMAD4 Is Indispensable for Febrile-Temperature-Mediated Th17 Cell Differentiation *In Vivo* and Associated Autoimmunity

To further investigate whether Smad4 is involved in regulating fever-dependent Th17 cell differentiation *in vivo*, we mixed naive CD45.1$^+$CD45.2$^+$ *Smad4*$^{fl/+}$ (WT) T cells and CD45.2$^+$ *Smad4*$^{fl/fl}$*Cd4*^{Cre} (*Smad4*$^{-/-}$) T cells both carrying the MOG-specific 2D2 TcR transgene at 1:1 ratio and transferred them into *Tcrbd*$^{-/-}$ mice, followed by MOG+CFA immunization. SMAD4 deficiency did not alter the ratio of T cells in recipient mice and significantly reduced the expression of IL-17A but not interferon-γ (IFN-γ) (Figure 6A). Importantly, treatment with anti-pyretic drug significantly reduced IL-17A expression in WT 2d2$^+$ T cells, down to an amount similar to *Smad4*$^{-/-}$ 2d2$^+$ T cells, but barely affected IL-17A expression in *Smad4*$^{-/-}$ 2d2$^+$ T cells (Figure 6A). These data together thus demonstrated an indispensable role of *Smad4* in regulating Th17 response *in vivo*.

To validate the above results, we conducted an active EAE model in *Smad4*$^{fl/fl}$ (WT) and *Smad4*$^{fl/fl}$ x *Cd4*^{Cre} (*Smad4*$^{\Delta CD4}$) mice (Figure S5A). *Smad4*$^{\Delta CD4}$mice showed delayed disease onset and greatly reduced disease scores (Figure 6B). IL-17$^+$ T cells were reduced in the CNS in these mice when compared with WT mice, whereas the IFN-γ$^+$ and FOXP3$^+$ T cells were comparable between two groups of mice (Figures 6C). To further examine if SMAD4 regulation of EAE requires its SUMOylation, we infected *Smad4*$^{-/-}$ 2d2$^+$ T cells with retroviruses containing either WT or the K113R/159R mutant *Smad4* under neutral culture condition (anti-IL-4 + anti-IFN-γ), and the infected T cells (GFP$^+$ cells) were sorted and introduced into *Rag1*$^{-/-}$ mice, followed by MOG immunization for induction of EAE diseases. Consistent with the EAE model performed with WT and *Smad4*$^{\Delta CD4}$ mice, mice receiving the *Smad4-K113R/159R*-transduced 2d2$^+$ T cells developed less severe diseases (Figure 6D), with reduced Th17 cells in the CNS, compared with those receiving WT *Smad4*-transduced T cells (Figure 6E).

The above studies demonstrated a pathogenic role of *Smad4* in EAE diseases via regulating Th17 cell differentiation. To investigate whether fever could regulate autoimmune diseases via similar pathways, EAE diseases were induced in WT and *Smad4*$^{\Delta CD4}$ mice treated with or without aspirin. Similar to SMAD4 deficiency, aspirin treatment reduced EAE diseases, as well as the percentages of CNS-infiltrating IL-17$^+$ T cells, but not those of FOXP3$^+$ Treg cells in WT mice (Figures S6A–S6C). However, aspirin treatment could not reduce Th17 cells in *Smad4*$^{\Delta CD4}$ mice (Figure S6C), again supporting a role of fever in regulating Th17 cell response *in vivo* via a SMAD4-dependent manner. In addition, aspirin could further reduce EAE diseases in *Smad4*$^{\Delta CD4}$ mice, indicating it may affect EAE diseases in both Th17-intrinsic and Th17-extrinsic manners, because of complex effects.

SMAD4 Orchestrates Febrile-Temperature-Associated Gene Expression at Genome-Wide Level

To examine the SMAD4-downstream regulated genes, RNA-seq assays were performed with WT and *Smad4*$^{-/-}$ Th17 cells induced at both 37°C and 39.5°C. DEG2 analysis showed over 5,000 genes were differentially expressed ($p < 0.01$, fold change ≥ 1), clustered into 4 groups (Figure 7A). Group 1 and group 3 represent genes most highly expressed or repressed at 39.5°C, respectively, dependent on *Smad4* (Figure 7A). In contrast, groups 2 and 4 represent genes most highly repressed or expressed at 37°C, respectively, also regulated by *Smad4* (Figure 7A). We then focused on the genes with ≥ 1.5-fold difference between 37°C and 39.5°C. Among the 1,083 genes induced at

Figure 5. SMAD4 Regulated Febrile Th17 Cell Differentiation in a SUMOylation-Dependent Manner

(A) Naive CD4$^+$ T cells were polarized with complete Th17 cell condition (IL-6+TGF-β1), IL-6-only condition (αTGF-β+IL-6), or TGF-β1-only condition at 37°C and 39.5°C for 24 h. The cells were collected, spun down to a cytospin microscope slide, and fixed and stained with αSMAD4 followed by staining with Alexa Fluor 488 conjugated secondary antibody. The cellular distribution of SMAD4 was visualized using a confocal fluorescence microscopy. The results shown here represent the merged photos of SMAD4 (green) and DAPI (blue, indicated for nuclear location) staining. Right: statistic data of SMAD4 nuclear translocation ratio, which was determined by manually counting the percentage of cells containing higher SMAD4 staining intensity in the nucleus versus cytoplasm in three representative fields revealed by Image-Pro Plus software. The results shown here represent one of the two independent experiments. The statistics were performed by Student's t test. *$p < 0.05$; **$p < 0.01$; ***$p < 0.001$.

(B) *Smad4*$^{-/-}$ naive T cells were activated under neutral condition at 37°C and infected with retrovirus harboring WT Smad4 or the K113R/159R mutant *Smad4* gene, and then polarized under Th17 cell culture condition (IL-6+TGF-β1) at 37°C or 39.5°C for reconstituting febrile Th17 cell differentiation. Intracellular staining of IL-17 data were gated on GFP$^+$ cells infected with retroviruses. The results shown here represent one of the two independent experiments.

(C) Immunofluorescence staining data of SMAD4 (red) in Th17 polarizing cultures (24 h post-retrovirus infection) as shown in (B). Left: immunofluorescence staining data (merged photo; GFP signal represents retrovirally infected cells, and blue DAPI staining represents nuclear location). Right: quantification data of SMAD4 nuclear translocation ratio. The statistics were performed by Student's t test. *$p < 0.05$; **$p < 0.01$; ***$p < 0.001$.

See also Figure S5.

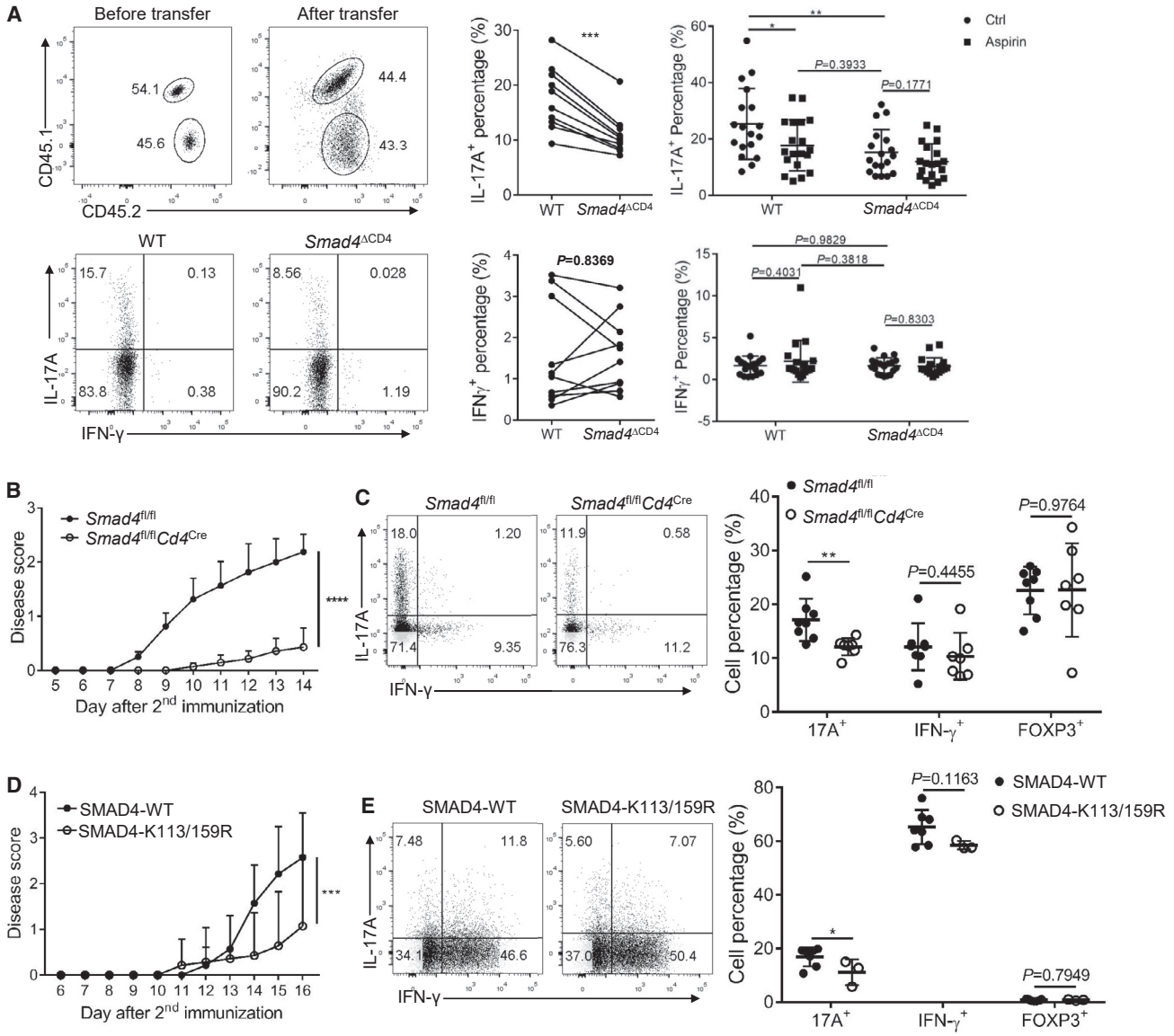

Figure 6. SMAD4 Deficiency Resulted in Defective Th17 Cell Differentiation *In Vivo* and Resistance to EAE

(A) Adoptive T cell transfer experiment: WT 2d2$^+$ (CD45.1$^+$CD45.2$^+$*Smad4*$^{fl/+}$) and *Smad4*$^{-/-}$ 2d2$^+$ (CD45.2$^+$*Smad4*$^{fl/fl}$*CD4*^{Cre}) naive T cells were mixed together at 1:1 ratio and transferred into *Tcrbd*$^{-/-}$ mice followed by MOG$_{35-55}$ immunization, and the donor cells were isolated from draining lymph nodes and analyzed 7 days later (n = 10). When indicated, the mice were treated with aspirin or control solution (0.5% methyl cellulose) by oral gavage at a dose of 2 mg/kg body weight twice a day for 7 days after immunization. Left: intracellular staining of the CD45.1 and CD45.2 congenic markers, IL-17 and IFN-γ in donor cells. Middle: statistic data of the left staining data. Right: statistic data of IL-17 and IFN-γ expression in the WT 2d2 and *Smad4*$^{-/-}$ 2d2 mixed T cell co-transfer experiment followed by aspirin or control treatment. The statistic data shown here represent a combination of three independent experiments, and analyzed by Student's t test. *p < 0.05; **p < 0.01; ***p < 0.001.

(B) Clinical EAE scores in WT (n = 8) and Smad4$^{-/-}$ (n = 7) mice after second MOG$_{35-55}$ immunization, and the difference in disease scores were analyzed by two-way ANOVA analysis (****indicate that the statistic p values for Smad4 genetic, and time factors are less than 0.0001).

(C) Left: intracellular staining IL-17 and IFN-γ in CD4$^+$ T cells infiltrated in the CNS of EAE mice. Right: statistic data of IL-17$^+$, IFN-γ$^+$, and FOXP3$^+$ T cells in percentages in the CNS as determined by Student's t test (*p < 0.05; **p < 0.01). The EAE experiments were repeated three times with consistent results.

(D and E) *Smad4*$^{\Delta CD4}$ (*Smad4*$^{fl/fl}$*Cd4Cre*) 2D2$^+$ T cells were first retrovirally infected with WT *Smad4* or the K113/159R mutant *Smad4*, and then adoptively transferred into *Rag1*$^{-/-}$ mice (n = 6–7 for each group) followed by MOG$_{35-55}$ immunization to induce EAE disease. The CNS-infiltrating T cells were then isolated from the CNS and analyzed for IL-17A and IFN-γ expression. (D) Clinical EAE scores in *Rag1*$^{-/-}$ mice receiving *Smad4*-WT and *Smad4-K113/159R* transduced T cells followed second MOG$_{35-55}$ immunization. The difference in disease scores were analyzed by two-way ANOVA analysis (***indicate that the statistic p values for Smad4 genetic, and time factors are less than 0.001). (E) Left: intracellular staining of IL-17A and IFN-γ in T cells infiltrated in the CNS. Right: statistic data of IL-17$^+$ and IFN-γ$^+$ T cells in percentages in the CNS as determined by Student's t test (*p < 0.05). Shown here represents one of the two independent transfer EAE results.

See also Figure S6.

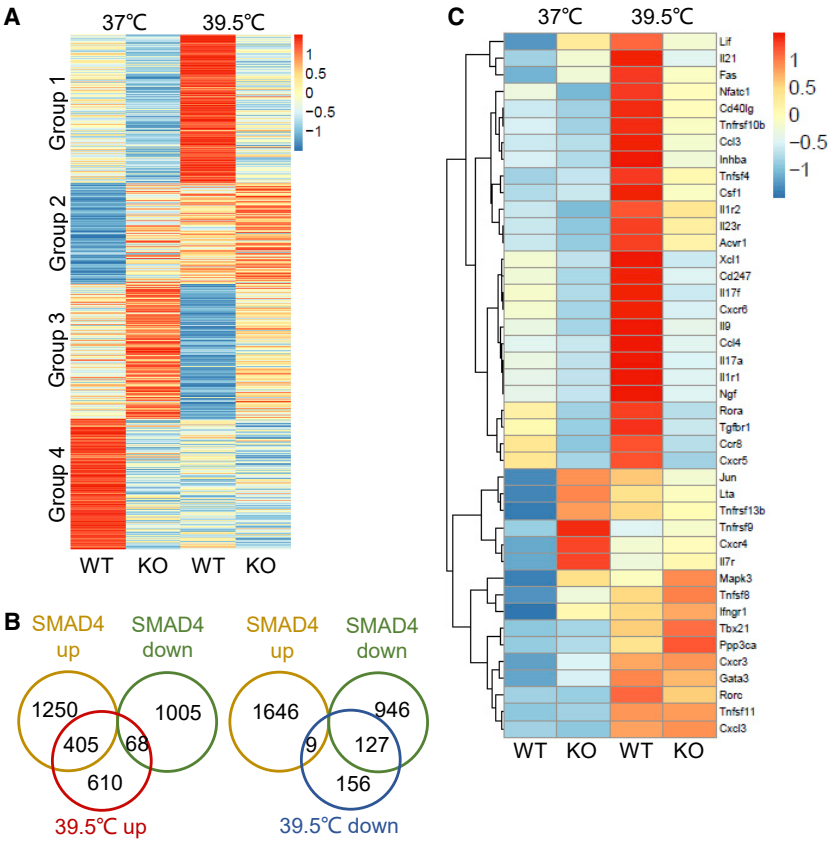

Figure 7. Smad4 Orchestrated the Differentiation and Pathogenicity of Th17 Cells

WT (*Smad4*$^{fl/fl}$) and *Smad4*$^{\Delta CD4}$ (*Smad4*$^{fl/fl}$*Cd4*^{Cre}) Th17 cells induced at 37°C or 39.5°C with IL-6 and TGF-β1 for 3 days were collected and used for whole-genome transcriptome analysis.

(A) Heatmap of genome-wide, differentially expressed genes in WT and *Smad4*$^{\Delta CD4}$ Th17 cells induced at 37°C and 39.5°C.

(B) Overlap of Smad4 upregulated or downregulated genes versus the genes induced (left) or repressed (right) at 39.5°C, respectively.

(C) Heatmap of 42 genes of febrile temperature induced genes enriched in the "Th17 cell differentiation" and "cytokine-cytokine interaction" pathways (≥1.5-fold upregulation).

See also Figure S7.

39.5°C, 405 were dependent on *Smad4* (Figure 7B). Among the 392 genes repressed at 39.5°C, 127 were regulated by *Smad4* (Figure 7B). Kyoto Encyclopedia of Genes and Genomes (KEGG) analysis showed that Th17 cell differentiation and cytokine-cytokine receptor interaction pathways are among the top listed pathways upregulated by febrile temperature (Figure S3A), which include 42 genes; 30 of the genes showed a strong *Smad4* dependence at 39.5°C but were largely unaffected by *Smad4* at 37°C, including genes critical for the differentiation and effect function of Th17 cells, such as *Il17a*, *Il17f*, *Il21, Il1r1*, *Il23r*, *Tbx21*, *Nfatc1*, etc. (Figure 7C). Moreover, GSEA revealed that *Smad4*-regulated gene expression patterns were more similar to Th17 cells from EAE than from the gut under steady status (Figure S5B). These data further confirm the necessary role of *Smad4* in regulating the pathogenicity of febrile Th17 cells.

To characterize the direct targets of *Smad4* in Th17 cells, genome-wide SMAD4 ChIP-seq assay was performed with Th17 cells induced at 37°C and 39.5°C. In total, SMAD4 bound ~2,000–2,200 gene loci in both types of Th17 cells, with ~40% (820 genes) in common (Figure S7A), indicating the transcriptional activity of Smad4 was altered in response to temperature. The 1,083 genes upregulated by febrile temperature were then overlaid with SMAD44 ChIP-seq data; among these, 145 had SMAD4 binding peaks at their gene loci, and only 60 showed increased binding at 39.5°C versus 37°C, including *Il17a*, *Il17f*, and *Nr4a2*, as well as *Gpr65*, which encodes a G-protein coupled receptor important for Th17 cell differentiation and EAE induction (Gaublomme et al., 2015) (Figure S7A). The increased binding of SMAD4 to *Il17a*, *Gpr65*, and *Nr4a2* were further confirmed by ChIP-PCR analysis (Figure S7B), indicating that SMAD4 regulates Th17 differentiation at febrile temperatures, likely through direct binding to the target gene loci.

DISCUSSION

A large body of our current knowledge on immunology is derived from *in vitro* studies performed at normal body temperature (37°C), which cannot fully mimic real physiological settings *in vivo* where fever is a common phenomenon in various infectious and immune-related diseases. In this study, we examined the effect of febrile temperature on T helper cell responses and found only Th17 cell differentiation was enhanced by elevated temperature. Febrile-temperature-induced Th17 cell differentiation relies on HSP70- and HSP90-related heat shock response and the protein SUMOylation pathway, specifically via SMAD4 SUMOylation, which was not observed in T cells cultured under Th1, Th2, and iTreg cell conditions (data not shown). As a result, T cells with SMAD4 deficiency or defects in SMAD4-SUMOylation failed in upregulating IL-17 expression at febrile temperatures and caused significantly reduced EAE diseases. Our study thus highlights an essential yet previously unappreciated role of fever in orchestrating Th17 cell response and related autoimmune diseases. On the other hand, fever-driven Th17 cell response might also benefit host protective immune response, particularly when considering the importance of Th17 cells in mucosal immunity in clearance of fungal and extracellular bacterial infections (Stockinger and Omenetti, 2017).

In contrast to the general notion on the role of fever in innate immunity, its function in adaptive immune response is much less understood. A few studies suggest fever may boost Th1 cell polarization (Hatzfeld-Charbonnier et al., 2007) and cytotoxic activity or tumor-killing abilities of CD8$^+$ T cells through potentiating their adhesion with antigen-presenting cells (Mace et al., 2011). Others suggest that fever can directly or indirectly promote T cell trafficking through activating α4-intergrin- or L-selectin-dependent adhesion and transmigration process (Evans

et al., 2000; Evans et al., 2001; Lin et al., 2019). It has been long recognized that blocking α4 integrin is effective in treatment of EAE diseases (Yednock et al., 1992), and natalizumab, a humanized monoclonal antibody against α4 integrin, has been developed and approved for treatment of multiple sclerosis (Miller et al., 2003; Tubridy et al., 1999). Consistently, anti-pyretic drugs, including celecoxib, rofecoxib, lumiracoxib, and aspirin, have been shown to also reduce immune-cell infiltration in the CNS in EAE models and alleviate disease symptoms, despite previous studies that suggest a possible direct effect of anti-pyretic drugs on *ex vivo* MBP- or MOG-specific T cell response (Miyamoto et al., 2006; Mondal et al., 2018; Ni et al., 2007). In this study, we showed that the physiological environment for Th17 cell differentiation *in vivo*, specifically in the draining lymph nodes and inflamed tissues, underwent temperature increase in inflammatory responses. Treatment with anti-fever drugs effectively reduced Th17 cell response *in vivo*, while Th17 cells generated *in vitro* at febrile temperatures were highly proinflammatory in a lung-inflammation model in striking similarity to those generated *in vivo* in the EAE model (Gaublomme et al., 2015). In addition, our experiments identified SMAD4 as the crucial fever-activated factor controlling febrile Th17 cell differentiation, and its deficiency dampens induction of EAE diseases in mice. These findings thus provide a direct link connecting fever to autoimmune diseases through Th17 cell responses. However, different from treatment with anti-pyrogenic drugs, SMAD4 deficiency did not affect the frequencies or numbers of $CD4^+$ T cells infiltrating into the CNS in the EAE model, nor IFN-γ^+ Th1 or $FOXP3^+$ Treg cell populations, suggesting that fever could affect inflammation via the SMAD4→Th17 axis, in addition to its role in mobilizing lymphocyte trafficking.

This study identifies SMAD4 as a positive regulator during Th17 cell differentiation at febrile temperatures, which is in contrast to our previous finding at normal temperature that *Smad4* is dispensable for Th17 cell differentiation (Yang et al., 2008) or a recent finding that SMAD4 inhibits IL-6-induced Th17 program via recruiting a transcription repressor, SKI (Zhang et al., 2017). In our current experiments, we confirmed all the previous findings under 37°C culture, and we also found that SMAD4 inhibited IL-6-induced Th17 cell program at 39.5°C. These results thus suggest that the function of SMAD4 is dependent on environmental cytokines and temperatures. At normal temperature and in the absence of TGF-β, it serves as a suppressor to limit unfavorable Th17 cell response through recruiting transcription repressor, SKI. Under Th17 cell-favorable conditions, the presence of TGF-β relieves SMAD4-dependent transcription repression via inducing SKI degradation (Zhang et al., 2017). However, because of mostly cytoplasmic localization, SMAD4 is non-functional under normal temperature. It becomes a transcriptional activator under fever condition as a result of its hyper-SUMOylation and increased nuclear localization.

Transcriptomes of WT and $Smad4^{\Delta CD4}$ Th17 cells generated at two different temperatures revealed that most fever-responsive genes, particularly those highly induced or repressed at febrile temperature, were largely dependent on *Smad4* for their expression, and in a total of 1,475 temperature sensitive genes (1,083 upregulated and 392 downregulated genes), 527 (~36%) are dependent on SMAD4, suggesting a global effect of *Smad4* in mediating T cell response at febrile temperatures. SMAD4-regulated genes include many key Th17-related pathogenic genes, such as *Il17*, *Il17f*, *Il21*, *Il1r1*, *Il1r2*, *Il23r*, *Tbx21*, and *Nr4a2,* and many are directly bound by SMAD4, supporting a direct regulation by the fever→SMAD4 axis. SMAD4 is known as a SUMO-targeted protein, and its SUMOylation at the K113 and K159 residues is required for nuclear localization and transcriptional activity (Lin et al., 2003). Similarly, febrile temperature increases both SMAD4 SUMOylation and its nuclear localization in Th17 cells. Based on these results, we would like to propose that SMAD4 does not regulate Th17 cell differentiation at 37°C because of its quick shuttling out of nuclei. At 39.5°C, SUMOylation results in increased SMAD4 nuclear localization and its binding at genes associated with Th17 cell pathogenicity. SUMOylation thus serves as a master switch with SMAD4 as the major downstream regulator in response to different temperatures.

In an EAE model, $Smad4^{\Delta CD4}$ mice exhibited greatly alleviated disease symptoms and delayed disease onset compared with WT mice, as well as a significant reduction in Th17 cells in the CNS. This finding is in contrast with a previous report that SMAD4 deficiency did not affect EAE disease (Zhang et al., 2017). However, a careful examination of their data clearly indicates a delayed onset of EAE disease and a reduced trend of disease scores in their $Smad4^{\Delta CD4}$ mice, at least at the early phase in their EAE model (≥2-fold difference in disease scores). Moreover, we used two times of immunization with MOG+CFA in our experiment, which may prolong the fever response in mice and amplify the effects of SMAD4. In addition, our T cell co-transfer experiments consistently support an important role of *Smad4* in regulating Th17 cell differentiation *in vivo* and related inflammatory response.

In summary, we show that febrile-range temperature could directly and selectively promote Th17 cell differentiation and provide direct evidence that Th17 cells generated under increased temperature are indeed more pro-inflammatory. Together, our *in vitro* and *in vivo* findings offer not only an insight into the pathogenic mechanisms underlying Th17 cell related autoimmune diseases but also provide an explanation on distinct transcriptional features between *in vitro*- and *in vivo*-generated Th17 cells under various physiological settings, revealed in previous reports (Gaublomme et al., 2015; Ghoreschi et al., 2010; Lee et al., 2012). This mechanism of regulation may be targeted in human autoimmune diseases.

STAR★METHODS

Detailed methods are provided in the online version of this paper and include the following:

- KEY RESOURCES TABLE
- LEAD CONTACT AND MATERIALS AVAILABILITY
- EXPERIMENTAL MODEL AND SUBJECT DETAILS
  - Mice
- METHOD DETAILS
  - Plasmid construction and retroviral transduction
  - *In vitro* T cells differentiation and flow cytometry
  - Acute lung inflammation model
  - Adoptive T cell transfer assay and EAE model

- Cytospin and immunofluorescence staining
- SUMOylation assay
- ChIP-seq
- RNA-seq
- Real-time PCR
- QUANTIFICATION AND STATISTICAL ANALYSIS
- DATA AND CODE AVAILABILITY

SUPPLEMENTAL INFORMATION

Supplemental Information can be found online at https://doi.org/10.1016/j.immuni.2020.01.006.

ACKNOWLEDGMENTS

We thank all the Dong lab members for their help. This work was supported by grants from the National Key Research and Development Program of China (2016YFC0906200 to C.D.), the National Natural Science Foundation of China (31630022, 31991173, 31821003, and 91642201 to C.D.; 31570884 to X.W.), Beijing Municipal Commission of Science and Technology, China (Z181100001318007, Z181100006318015, and Z171100000417005 to C.D.), and Beijing Natural Science Foundation, China (5172017 to X.W.).

AUTHOR CONTRIBUTIONS

C.D. supervised the project. X.W. started the project and found febrile temperature selectively enhanced Th17 cell differentiation. L.N. identified Smad4 as the major heat-responsive regulator. L.N. performed the experiments and analyzed data including GSEA. S.W. helped in the animal studies. X.D. helped in the SUMOylation studies. X.Z. analyzed the RNA-seq and ChIP-seq data. A.D. generated Ubc9fl/fl mice. L.N. wrote the original draft. X.W. and C.D. revised the manuscript.

DECLARATION OF INTERESTS

X.W., C.D., and L.N. have filed a patent application on the role of febrile temperatures in IL-17 producing T cells.

Received: June 17, 2019
Revised: October 2, 2019
Accepted: January 19, 2020
Published: February 11, 2020

REFERENCES

Bai, X.F., Liu, J.Q., Liu, X., Guo, Y., Cox, K., Wen, J., Zheng, P., and Liu, Y. (2000). The heat-stable antigen determines pathogenicity of self-reactive T cells in experimental autoimmune encephalomyelitis. J. Clin. Invest. *105*, 1227–1232.

Bettelli, E., Sullivan, B., Szabo, S.J., Sobel, R.A., Glimcher, L.H., and Kuchroo, V.K. (2004). Loss of T-bet, but not STAT1, prevents the development of experimental autoimmune encephalomyelitis. J. Exp. Med. *200*, 79–87.

Chitnis, T., Najafian, N., Benou, C., Salama, A.D., Grusby, M.J., Sayegh, M.H., and Khoury, S.J. (2001). Effect of targeted disruption of STAT4 and STAT6 on the induction of experimental autoimmune encephalomyelitis. J. Clin. Invest. *108*, 739–747.

Chu, G.C., Dunn, N.R., Anderson, D.C., Oxburgh, L., and Robertson, E.J. (2004). Differential requirements for Smad4 in TGFbeta-dependent patterning of the early mouse embryo. Development *131*, 3501–3512.

Demarque, M.D., Nacerddine, K., Neyret-Kahn, H., Andrieux, A., Danenberg, E., Jouvion, G., Bomme, P., Hamard, G., Romagnolo, B., Terris, B., et al. (2011). Sumoylation by Ubc9 regulates the stem cell compartment and structure and function of the intestinal epithelium in mice. Gastroenterology *140*, 286–296.

Doi, Y., Oki, S., Ozawa, T., Hohjoh, H., Miyake, S., and Yamamura, T. (2008). Orphan nuclear receptor NR4A2 expressed in T cells from multiple sclerosis mediates production of inflammatory cytokines. Proc. Natl. Acad. Sci. USA *105*, 8381–8386.

Eming, S.A., Wynn, T.A., and Martin, P. (2017). Inflammation and metabolism in tissue repair and regeneration. Science *356*, 1026–1030.

Esplugues, E., Huber, S., Gagliani, N., Hauser, A.E., Town, T., Wan, Y.Y., O'Connor, W., Jr., Rongvaux, A., Van Rooijen, N., Haberman, A.M., et al. (2011). Control of TH17 cells occurs in the small intestine. Nature *475*, 514–518.

Evans, S.S., Bain, M.D., and Wang, W.C. (2000). Fever-range hyperthermia stimulates alpha4beta7 integrin-dependent lymphocyte-endothelial adhesion. International journal of hyperthermia: the official journal of European Society for Hyperthermic Oncology. International Journal of Hyperthermia *16*, 45–59.

Evans, S.S., Wang, W.C., Bain, M.D., Burd, R., Ostberg, J.R., and Repasky, E.A. (2001). Fever-range hyperthermia dynamically regulates lymphocyte delivery to high endothelial venules. Blood *97*, 2727–2733.

Evans, S.S., Repasky, E.A., and Fisher, D.T. (2015). Fever and the thermal regulation of immunity: the immune system feels the heat. Nat. Rev. Immunol. *15*, 335–349.

Gareau, J.R., and Lima, C.D. (2010). The SUMO pathway: emerging mechanisms that shape specificity, conjugation and recognition. Nat. Rev. Mol. Cell Biol. *11*, 861–871.

Gaublomme, J.T., Yosef, N., Lee, Y., Gertner, R.S., Yang, L.V., Wu, C., Pandolfi, P.P., Mak, T., Satija, R., Shalek, A.K., et al. (2015). Single-Cell Genomics Unveils Critical Regulators of Th17 Cell Pathogenicity. Cell *163*, 1400–1412.

Ghoreschi, K., Laurence, A., Yang, X.P., Tato, C.M., McGeachy, M.J., Konkel, J.E., Ramos, H.L., Wei, L., Davidson, T.S., Bouladoux, N., et al. (2010). Generation of pathogenic T(H)17 cells in the absence of TGF-β signalling. Nature *467*, 967–971.

Hahn, J.N., Falck, V.G., and Jirik, F.R. (2011). Smad4 deficiency in T cells leads to the Th17-associated development of premalignant gastroduodenal lesions in mice. J. Clin. Invest. *121*, 4030–4042.

Hansen, W., Loser, K., Westendorf, A.M., Bruder, D., Pfoertner, S., Siewert, C., Huehn, J., Beissert, S., and Buer, J. (2006). G protein-coupled receptor 83 overexpression in naive CD4+CD25- T cells leads to the induction of Foxp3+ regulatory T cells in vivo. J. Immunol. *177*, 209–215.

Hasday, J.D., Thompson, C., and Singh, I.S. (2014). Fever, immunity, and molecular adaptations. Compr. Physiol. *4*, 109–148.

Hatzfeld-Charbonnier, A.S., Lasek, A., Castera, L., Gosset, P., Velu, T., Formstecher, P., Mortier, L., and Marchetti, P. (2007). Influence of heat stress on human monocyte-derived dendritic cell functions with immunotherapeutic potential for antitumor vaccines. J. Leukoc. Biol. *81*, 1179–1187.

Jiang, Y., Liu, Y., Lu, H., Sun, S.C., Jin, W., Wang, X., and Dong, C. (2018). Epigenetic activation during T helper 17 cell differentiation is mediated by Tripartite motif containing 28. Nat. Commun. *9*, 1424.

Kleinewietfeld, M., Manzel, A., Titze, J., Kvakan, H., Yosef, N., Linker, R.A., Muller, D.N., and Hafler, D.A. (2013). Sodium chloride drives autoimmune disease by the induction of pathogenic TH17 cells. Nature *496*, 518–522.

Langmead, B., and Salzberg, S.L. (2012). Fast gapped-read alignment with Bowtie 2. Nat. Methods *9*, 357–359.

Lee, P.P., Fitzpatrick, D.R., Beard, C., Jessup, H.K., Lehar, S., Makar, K.W., Pérez-Melgosa, M., Sweetser, M.T., Schlissel, M.S., Nguyen, S., et al. (2001). A critical role for Dnmt1 and DNA methylation in T cell development, function, and survival. Immunity *15*, 763–774.

Lee, Y., Awasthi, A., Yosef, N., Quintana, F.J., Xiao, S., Peters, A., Wu, C., Kleinewietfeld, M., Kunder, S., Hafler, D.A., et al. (2012). Induction and molecular signature of pathogenic TH17 cells. Nat. Immunol. *13*, 991–999.

Li, P., Zheng, Y., and Chen, X. (2017). Drugs for Autoimmune Inflammatory Diseases: From Small Molecule Compounds to Anti-TNF Biologics. Front. Pharmacol. *8*, 460.

Limper, M., de Kruif, M.D., Duits, A.J., Brandjes, D.P., and van Gorp, E.C. (2010). The diagnostic role of procalcitonin and other biomarkers in discriminating infectious from non-infectious fever. J. Infect. *60*, 409–416.

Lin, X., Liang, M., Liang, Y.Y., Brunicardi, F.C., and Feng, X.H. (2003). SUMO-1/Ubc9 promotes nuclear accumulation and metabolic stability of tumor suppressor Smad4. J. Biol. Chem. *278*, 31043–31048.

Lin, C., Zhang, Y., Zhang, K., Zheng, Y., Lu, L., Chang, H., Yang, H., Yang, Y., Wan, Y., Wang, S., et al. (2019). Fever Promotes T Lymphocyte Trafficking via a Thermal Sensory Pathway Involving Heat Shock Protein 90 and alpha4 Integrins. Immunity *50*, 137–151.

Mace, T.A., Zhong, L., Kilpatrick, C., Zynda, E., Lee, C.T., Capitano, M., Minderman, H., and Repasky, E.A. (2011). Differentiation of CD8+ T cells into effector cells is enhanced by physiological range hyperthermia. J. Leukoc. Biol. *90*, 951–962.

Malhotra, N., Robertson, E., and Kang, J. (2010). SMAD2 is essential for TGF beta-mediated Th17 cell generation. J. Biol. Chem. *285*, 29044–29048.

Martinez, G.J., Zhang, Z., Chung, Y., Reynolds, J.M., Lin, X., Jetten, A.M., Feng, X.H., and Dong, C. (2009). Smad3 differentially regulates the induction of regulatory and inflammatory T cell differentiation. J. Biol. Chem. *284*, 35283–35286.

Martinez, G.J., Zhang, Z., Reynolds, J.M., Tanaka, S., Chung, Y., Liu, T., Robertson, E., Lin, X., Feng, X.H., and Dong, C. (2010). Smad2 positively regulates the generation of Th17 cells. J. Biol. Chem. *285*, 29039–29043.

Miller, D.H., Khan, O.A., Sheremata, W.A., Blumhardt, L.D., Rice, G.P., Libonati, M.A., Willmer-Hulme, A.J., Dalton, C.M., Miszkiel, K.A., and O'Connor, P.W.; International Natalizumab Multiple Sclerosis Trial Group (2003). A controlled trial of natalizumab for relapsing multiple sclerosis. N. Engl. J. Med. *348*, 15–23.

Miyamoto, K., Miyake, S., Mizuno, M., Oka, N., Kusunoki, S., and Yamamura, T. (2006). Selective COX-2 inhibitor celecoxib prevents experimental autoimmune encephalomyelitis through COX-2-independent pathway. Brain *129*, 1984–1992.

Mondal, S., Jana, M., Dasarathi, S., Roy, A., and Pahan, K. (2018). Aspirin ameliorates experimental autoimmune encephalomyelitis through interleukin-11-mediated protection of regulatory T cells. Sci. Signal. *11*, eaar8278.

Ni, J., Shu, Y.Y., Zhu, Y.N., Fu, Y.F., Tang, W., Zhong, X.G., Wang, H., Yang, Y.F., Ren, J., Wang, M.W., and Zuo, J.P. (2007). COX-2 inhibitors ameliorate experimental autoimmune encephalomyelitis through modulating IFN-gamma and IL-10 production by inhibiting T-bet expression. J. Neuroimmunol. *186*, 94–103.

Pasikhova, Y., Ludlow, S., and Baluch, A. (2017). Fever in Patients With Cancer. Cancer control: journal of the Moffitt Cancer Center *24*, 193–197.

Reppert, S., Zinser, E., Holzinger, C., Sandrock, L., Koch, S., and Finotto, S. (2015). NFATc1 deficiency in T cells protects mice from experimental autoimmune encephalomyelitis. Eur. J. Immunol. *45*, 1426–1440.

Saitoh, H., and Hinchey, J. (2000). Functional heterogeneity of small ubiquitin-related protein modifiers SUMO-1 versus SUMO-2/3. J. Biol. Chem. *275*, 6252–6258.

Shang, J., Yan, L., Du, L., Liang, L., Zhou, Q., Liang, T., Bai, L., and Tang, H. (2017). Recent trends in the distribution of causative diseases of fever of unknown origin. Wien. Klin. Wochenschr. *129*, 201–207.

Singh, I.S., and Hasday, J.D. (2013). Fever, hyperthermia and the heat shock response. Int. J. Hyperthermia *29*, 423–435.

Stockinger, B., and Omenetti, S. (2017). The dichotomous nature of T helper 17 cells. Nat. Rev. Immunol. *17*, 535–544.

Sugimoto, N., Oida, T., Hirota, K., Nakamura, K., Nomura, T., Uchiyama, T., and Sakaguchi, S. (2006). Foxp3-dependent and -independent molecules specific for CD25+CD4+ natural regulatory T cells revealed by DNA microarray analysis. Int. Immunol. *18*, 1197–1209.

Tubridy, N., Behan, P.O., Capildeo, R., Chaudhuri, A., Forbes, R., Hawkins, C.P., Hughes, R.A., Palace, J., Sharrack, B., Swingler, R., et al.; The UK Antegren Study Group (1999). The effect of anti-alpha4 integrin antibody on brain lesion activity in MS. Neurology *53*, 466–472.

Wang, L., Feng, Z., Wang, X., Wang, X., and Zhang, X. (2010). DEGseq: an R package for identifying differentially expressed genes from RNA-seq data. Bioinformatics *26*, 136–138.

Wang, X., Zhang, Y., Yang, X.O., Nurieva, R.I., Chang, S.H., Ojeda, S.S., Kang, H.S., Schluns, K.S., Gui, J., Jetten, A.M., and Dong, C. (2012). Transcription of Il17 and Il17f is controlled by conserved noncoding sequence 2. Immunity *36*, 23–31.

Wedepohl, S., Beceren-Braun, F., Riese, S., Buscher, K., Enders, S., Bernhard, G., Kilian, K., Blanchard, V., Dernedde, J., and Tauber, R. (2012). L-selectin–a dynamic regulator of leukocyte migration. Eur. J. Cell Biol. *91*, 257–264.

Wu, C., Yosef, N., Thalhamer, T., Zhu, C., Xiao, S., Kishi, Y., Regev, A., and Kuchroo, V.K. (2013). Induction of pathogenic TH17 cells by inducible salt-sensing kinase SGK1. Nature *496*, 513–517.

Yang, X.O., Panopoulos, A.D., Nurieva, R., Chang, S.H., Wang, D., Watowich, S.S., and Dong, C. (2007). STAT3 regulates cytokine-mediated generation of inflammatory helper T cells. J. Biol. Chem. *282*, 9358–9363.

Yang, X.O., Nurieva, R., Martinez, G.J., Kang, H.S., Chung, Y., Pappu, B.P., Shah, B., Chang, S.H., Schluns, K.S., Watowich, S.S., et al. (2008). Molecular antagonism and plasticity of regulatory and inflammatory T cell programs. Immunity *29*, 44–56.

Yednock, T.A., Cannon, C., Fritz, L.C., Sanchez-Madrid, F., Steinman, L., and Karin, N. (1992). Prevention of experimental autoimmune encephalomyelitis by antibodies against alpha 4 beta 1 integrin. Nature *356*, 63–66.

Yu, G., Wang, L.G., Han, Y., and He, Q.Y. (2012). clusterProfiler: an R package for comparing biological themes among gene clusters. OMICS *16*, 284–287.

Yu, G., Wang, L.G., and He, Q.Y. (2015). ChIPseeker: an R/Bioconductor package for ChIP peak annotation, comparison and visualization. Bioinformatics *31*, 2382–2383.

Zhang, S. (2018). The role of transforming growth factor β in T helper 17 differentiation. Immunology *155*, 24–35.

Zhang, Y., Liu, T., Meyer, C.A., Eeckhoute, J., Johnson, D.S., Bernstein, B.E., Nusbaum, C., Myers, R.M., Brown, M., Li, W., and Liu, X.S. (2008). Model-based analysis of ChIP-Seq (MACS). Genome Biol. *9*, R137.

Zhang, S., Takaku, M., Zou, L., Gu, A.D., Chou, W.C., Zhang, G., Wu, B., Kong, Q., Thomas, S.Y., Serody, J.S., et al. (2017). Reversing SKI-SMAD4-mediated suppression is essential for T_H17 cell differentiation. Nature *551*, 105–109.

Zhu, Q., Wu, X., and Wang, X. (2017). Differential distribution of tumor-associated macrophages and Treg/Th17 cells in the progression of malignant and benign epithelial ovarian tumors. Oncol. Lett. *13*, 159–166.

Please cite this article in press as: Wang et al., Febrile Temperature Critically Controls the Differentiation and Pathogenicity of T Helper 17 Cells, Immunity (2020), https://doi.org/10.1016/j.immuni.2020.01.006

STAR★METHODS

KEY RESOURCES TABLE

REAGENT or RESOURCE	SOURCE	IDENTIFIER
Antibodies		
Anti-CD3 (clone 17A2)	Bioxcell	Cat# BE0002; RRID: AB_1107630
Anti-CD28 (clone 37.51)	Bioxcell	Cat# BE0015-1; RRID: AB_1107628
Anti-TGF-β	R&D Systems	Cat# MAB1835; RRID: AB_357931
Anti-SUMO2	Invitrogen	Cat# 519100; RRID: N/A
Anti-SMAD4	Santa Cruz	Cat# sc-7966; RRID: AB_627905
Anti-SMAD4	Abcam	Cat# ab40759; RRID: AB_777980
Anti-HSF1	cell signaling technology	Cat# 4356s; RRID: AB_2120258
Anti-HSF2	Santa Cruz	Cat# sc-13517; RRID: AB_627754
Anti-CD45.1	eBioscience	Cat#25-0453-81; RRID: AB_469628
Anti-CD45.2	eBioscience	Cat# 56-0454; RRID: AB_657753
Anti-CD11b	eBioscience	Cat# 25-0112-81; RRID: AB_469587
Anti-CD11c	eBioscience	Cat# 48-0114-82; RRID: AB_1548654
Anti-F4/80	Biolegend	Cat# 123110; RRID: AB_893486
Anti-Singlec-F	BD Biosciences	Cat# 562680; RRID: AB_2687570
Anti-Gr-1	eBioscience	Cat# 45-5931; RRID: AB_906247
Anti-IL-4	BD Biosciences	Cat# 554435; RRID: AB_395391
Anti-IL-13	eBioscience	Cat# 12-7133-81; RRID: AB_763561
Anti-IFN-γ	BD Biosciences	Cat# 557724; RRID: AB_396832
Anti-IL-17A	BD Biosciences	Cat# 559502; RRID: AB_397256
Anti-FOXP3	eBioscience	Cat# 48-5773-82; RRID: AB_1518812
Anti-Mouse IgG H&L	Abcam	ab46540; RRID: AB_2614925
Chemicals, Peptides, and Recombinant Proteins		
Fixable viability dye eFluor506	eBioscience	Cat# 65-0866
Albumin from chicken egg white (OVA)	Sigma	Cat# A5503
M. Tuberculosis Des. H37 Ra	BD	Cat# 231141
Freund's Adjuvant Incomplete	Sigma	F5506-100
Myelin Oligodendrocyte Glycoprotein	China Peptides	N/A
Recombinant Murine IL-6	Peprotech	Cat# 216-16
Recombinant Human TGF-beta	R&D Systems	Cat# 240-B-010
TRIzol	Invitrogen	Cat# 15596018
HSP90 inhibitor NMS-E973	Selleckchem	Cat#S7282
HSP70 inhibitor VER155008	Selleckchem	Cat#S7751
TGF-β RI inhibitor SB431542	Selleckchem	Cat# S1067
Aspirin	Selleckchem	Cat# S3017
Ibuprofen	Selleckchem	Cat# S1638
Methyl cellulose	Sigma	Cat# M0262
Critical Commercial Assays		
Fixation/Permeabilization Solution Kit	BD Biosciences	Cat# 554714
Foxp3 / Transcription Factor Staining Buffer Set	eBioscience	Cat# 00-5523-00
ChIP-IT Express Enzymatic Shearing Kit	Active Motif	Cat# 53035
CD4 (L3T4) MicroBeads, mouse	Miltenyi Biotec	Cat# 130-117-043
M-MLV Reverse Transcriptase	Promega	Cat# M5313
Hieff qPCR SYBR Green Master Mix	Yeasen	Cat# 11201ES03
Dynabeads Protein A	Life Technologies	Cat# 10002D

(*Continued on next page*)

Continued

REAGENT or RESOURCE	SOURCE	IDENTIFIER
Deposited Data		
Raw RNA-seq data	This study	GSE125264
Raw SMAD4 ChIP-seq data	This study	GSE125263
Experimental Models: Organisms/Strains		
Mouse: C57BL/6J	Jackson Laboratory	JAX:000664
Mouse: *CD4Cre* (B6.Cg-Tg(Cd4-cre)1Cwi/BfluJ)	Jackson Laboratory	Jax: 022071
Mouse: OT-II: B6.Cg-Tg(TcraTcrb)425Cbn/J	Jackson Laboratory	Jax: 4194
Mouse: CD45.1: B6.SJL-PtprcaPepcb/BoyJ	Jackson Laboratory	Jax: 002014
Mouse: CreERT2: B6.129-Gt(ROSA)26Sortm1(cre/ERT2)Tyj/J	Jackson Laboratory	Jax: 008463
Mouse: Smad4fl: Smad4tm2.1Cxd/J	Jackson Laboratory	Jax: 017462
Mouse: Ubc9fl	Dr. Anne Dejean's Lab	N/A
Oligonucleotides		
Clone primer: Smad4-WT Forward: CACGCGTTACTCCAGA AATTGGAGAGTTGGAT; Reverse: CGGAATTCTCAGTCTAA AGGCTGTGGGTC	This paper	N/A
Clone primer: Smad4-K113R Forward: AAGCATGTTAGATA TTGTCAG TATGCGTTTG; Reverse: CTGACAATATCTAACA TGCTTTAGTTCATTCTTGTG	This paper	N/A
Clone primer: Smad4-K159R Forward: ATGTTAGTGAGGG ATGAGTAC GTTCACGA; Reverse: GTACTCATCCCTCAC TAACATACTTGGAGC	This paper	N/A
Clone primer: shRNA-1 Forward: CCGGCGATTACTGTCA AGGTTATTTCTCGAGAAATAACCTTGACAGTAATCGTT TTTG; Reverse: AATTCAAAAACGATTACTGTCAAGGTT ATTTCTCGAGAAATAACCTTGACAGTAATCG	This paper	N/A
Clone primer: shRNA-2 Forward: CCGGTTATCTGCTTG TCCATGTTAACTCGAGTTAACATGGACAAGCAGATAA TTTTTG; Reverse: AATTCAAAAATTATCTGCTTGTCCA TGTTAACTCGAGTTAACATGGACAAGCAGATAA	This paper	N/A
Clone primer: RVKM-Hsp70 Forward: ATACGCGTCATGG CCAAGAACACGGC; Reverse: ATGAATTCCTAATCCACCT CCTCGATGGT	This paper	N/A
Real-time PCR primer: Il17a Forward: CTCCAGAAGGCCC TCAGACTAC; Reverse: GGGTCTTCATTGCGGTGG	This paper	N/A
Real-time PCR primer: Il17f Forward: CCCATGGGATTACA ACATCACTC; Reverse: CACTGGGCCTCAGCGATC	This paper	N/A
Real-time PCR primer: Rorc Forward: CACGGCCCTGGTT CTCAT; Reverse: CAGATGTTCCACTCTCCTCTTCTCT	This paper	N/A
Real-time PCR primer: Rora Forward: TCCAAATCCCACC TGGAAAC; Reverse: GGAAGGTCTGCCACGTTATCTG	This paper	N/A
Real-time PCR primer: Il22 Forward: CATGCAGGAGGTG GTACCTT; Reverse: CAGACGCAAGCATTTCTCAG	This paper	N/A
Real-time PCR primer: Il23r Forward: GCCAAGAGAACCA TTCCCGA; Reverse: TCAGTGCTACAATCTTCAGAGGACA	This paper	N/A
Real-time PCR primer: Il1r1 Forward: GTGCTACTGGGG CTCATTTGT; Reverse: GGAGTAAGAGGACACTTGCGAAT	This paper	N/A
Real-time PCR primer: Il1r2 Forward: GTTTCTGCTTTCAC CACTCCA; Reverse: GAGTCCAATTTACTCCAGGTCAG	This paper	N/A
Real-time PCR primer: Tgfbr1 Forward: TCTGCATTGCACT TATGCTGA; Reverse: AAAGGGCGATCTAGTGATGGA	This paper	N/A
Real-time PCR primer: Il10 Forward: ATAACTGCACCCAC TTCCCAGTC; Reverse: CCCAAGTAACCCTTAAAGTCCTGC	This paper	N/A

(*Continued on next page*)

Continued

REAGENT or RESOURCE	SOURCE	IDENTIFIER
Real-time PCR primer: Hsp40 Forward: ACCAGACCTCGA ACAACATTCC; Reverse: TAGGGACATTCACAGTGCAACC	This paper	N/A
Real-time PCR primer: Hsp60 Forward: GCACTGGCTCCTC ATCTCACTC; Reverse: CAACAGTGACCCCATCTTTTGT	This paper	N/A
Real-time PCR primer: Hsp70 Forward: AGGTGAACTACAA GGGCGAGAG; Reverse: CGCTGAGAGTCGTTGAAGTAGG	This paper	N/A
Real-time PCR primer: Hsp90aa Forward: AACCTTTGTTCCA CGACCCATT; Reverse: CTGCTCATCGTCGTTATGCTTC	This paper	N/A
Real-time PCR primer: Hsp90ab Forward: ATGGAGGAGAG CAAGGCAAAGT; Reverse: GCAGCAGGGTGAAGACACAAG	This paper	N/A
Real-time PCR primer: Hsp110 h Forward: ACCTCAAGAAG CCAGTGACAGA; Reverse: AAGCAGTTCAAGCCCACAATCT	This paper	N/A
ChIP-QPCR primer: Il17p Forward: CACCTCACACGAGGC ACAAG; Reverse: ATGTTTGCGCGTCCTGATC	This paper	N/A
ChIP-QPCR primer: Il17 Forward: TCACATGACGCTATGC AATGAGAA; Reverse: TTGGGATAAAGCAATGGATGAAAA	This paper	N/A
ChIP-QPCR primer: Gpr65 Forward: GTCCTTCCCTTCTTG TGGTTCAG; Reverse: GCACTGAAACCAGATGACAGACTG	This paper	N/A
ChIP-QPCR primer: Nr4a2 Forward: TAGTGTCGGTAGAGG GTCCTG; Reverse: CCGCCGCCCTTGAAAATATG	This paper	N/A
ChIP-QPCR primer: Il5 (negative control) Forward: TGAAG GCTAAAAGAAGGGCATCA; Reverse: GGAGAGATGGCTC AGTGGTTAAGA	This paper	N/A
Software and Algorithms		
FlowJo software v10.7	FlowJo	https://www.flowjo.com/
GSEA		http://software.broadinstitute.org/gsea/index.jsp
Prism 7	graphpad	https://www.graphpad.com
Image-Pro Plus 6.0	Media Cybernetics	https://image-pro-plus.updatestar.com/en
ImageJ	National Institutes of Health	https://imagej.nih.gov/ij/

LEAD CONTACT AND MATERIALS AVAILABILITY

Further information and requests for resources and reagents should be directed to and will be fulfilled by the Lead Contact, Chen Dong (chendong@tsinghua.edu.cn).

EXPERIMENTAL MODEL AND SUBJECT DETAILS

Mice

The *Smad4*$^{fl/fl}$ mice were previously described (Chu et al., 2004), and were crossed with *Cd4Cre* (Lee et al., 2001) to generated conditional *Smad4*$^{\Delta CD4}$ mice. The *Tcrbd*$^{-/-}$, *CreERT2*, *CD45.1*, *OT-II* TCR and 2D2 TCR transgenic mice were purchased from Jackson Laboratories. The 2D2 mice and CD45.1 were crossed with *Smad4*$^{fl/fl}$*Cd4*^{Cre} when indicated. The *Ubc9*$^{fl/fl}$ mice were previously described (Demarque et al., 2011), and were crossed with *CreERT2* mice for preparing inducible *Ubc9* ablated T cells. All the mice were housed in the SPF animal facility at Tsinghua University. All the animal experiments were performed according to the protocols approved by the Institutional Animal Care and Use Committee.

METHOD DETAILS

Plasmid construction and retroviral transduction

The WT *Smad4* gene (gene access ID: 17128) was PCR amplified using the primers below: CACGCGTTACTCCAGAAATTGGA GAGTTGGAT (forward) and CGGAATTCTCAGTCTAAAGGCTGTGGGTC (reverse), cloned into the pRVKM retroviral vector, and then used for constructing the Smad4-K113/159R mutant plasmid by site-direct mutagenesis. The Smad4 or control plasmids were transfected together with pcl-ECO into 293T cells for preparing retrovirus. Naive CD4^{+} T cells were activated with plate-bound anti-CD3 plus anti-CD28 for 24 h under neutral condition, and were infected with virus harboring the WT and Smad4 mutant genes by

spinning. The infected T cells were washed and changed to Th17 polarizing condition for additional two days cultured at 37°C or 39.5°C.

In vitro T cells differentiation and flow cytometry

$CD4^+$ T cells were isolated using MACS mouse $CD4^+$ T cell isolation kit (Miltenyi) and $CD4^+CD25^-CD44^{low}CD62L^{high}$ naive $CD4^+$ T cells were sorted by FACS Aria III cell sorter (BD). Naive $CD4^+$ T cells were cultured in RPMI 1640 medium (GIBCO) supplemented with 100 U/mL of penicillin, 100 μg/mL of streptomycin, 0.05 mM of β-mercaptoethanol and 10% fetal bovin serum (GIBCO) and differentiated in 48-well plates coated with 2 μg/mL αCD3 (BioXcell) and 2 μg/mL αCD28 (BioXcell) in the presence of different cytokine cocktails: Th1: IL-12 (15 ng/mL), IL-2 (25 U/mL) and αIL-4 (10 μg/mL); Th2: IL-4(20 ng/mL), IL-2 (25 U/mL), αIFN-γ (10 μg/mL); non-pathogenic Th17: IL-6 (15 ng/mL), TGF-β1 (2 ng/mL); pathogenic Th17: IL-6 (15 ng/mL), TGF-β1 (2 ng/mL), IL-23 (25 ng/mL), IL-1β (10 ng/mL); iTreg: TGF-β1 (2 ng/mL), IL-2 (25 U/mL).

For flow cytometry, the cells were re-suspended in 1xPBS for staining with fixable live/dead cell dye (eBioscience, Cat# 65-0866), followed by various surface markers as indicated, and then fixed using the eBioscience Fix/Perm or BD Fix/Perm buffer kit for intracellular staining of FOXP3, IFN-γ, IL-4, IL-13 or IL-17A as indicated, and finally analyzed with the LSR Fortessa cell analyzer (BD) and FlowJo software. For cytokine staining, the cells were first re-stimulated for 5 h in the presence of phorbol-12-myristate-13-acetate (50 ng/mL), ionomycin (500 ng/mL) and Golgi-stop (2 μM, BD Biosciences, Cat#554724) before staining. The cells obtained in *in vivo* models were blocked by αCD16/CD32 before staining, and the neutrophils were gated as $Gr1^+CD11b^+$ population

Acute lung inflammation model

Naive $CD4^+$ T cells were sorted from OT II mice and co-cultured with antigen presenting cells (APCs) (1:2 ratio) in the presence of OVA peptide (3 μg/mL) under neutral condition (αIFN-γ + αIL-4) for two days at 37°C, and the culture system was then changed to Th17 polarizing condition for another 3 days at 37°C or 39.5°C. One million OVA-specific Th17 cells were then transferred to CD45.1 congenic recipients followed by intra-nasal inhalation of OVA peptide (25 μg/mouse). The mice were then sacrificed and the BALF and lung tissue were then collected for further analysis according to previous studies.

Adoptive T cell transfer assay and EAE model

Naive T cells isolated from *CD45.1*$^+$ *CD45.2*$^+$*2d2*$^+$ *Smad4*$^{fl/+}$ ($CD45.1^+CD45.2^+$ WT) and *CD45.2*$^+$ *2d2*$^+$ *Smad4*$^{fl/fl}$ *CD4*^{Cre} ($CD45.2^+$ *Smad4*$^{\Delta CD4}$) mice were mixed at 1:1 ratio and transferred into the *Tcrbd*$^{-/-}$ recipient mice (1 million/mouse), followed by subcutaneous immunization at the tail base with MOG_{35-55} peptides emulsified in complete Freund's adjuvant (CFA). When indicated, the mice were treated by gavage with aspirin at 2 mg/kg body weight or ibuprofen in 0.5% methylcellulose twice a day throughout the experiment. The mice were sacrificed 7 days later and the draining lymph nodes were then collected for further analysis.

The active EAE was induced by subcutaneous immunization at the tail base with 150 μg/mice MOG_{35-55} peptides emulsified in 100 μL of complete Freund's adjuvant (CFA, 5 mg/mL) on day 1 and day 7, followed by i.p. injection of 500 μg/mice pertussis toxin dissolved in 1xPBS on day 2 and day 8. The disease was scored based on the following standards: 0, no clinical sign of disease; 1, loss of tail tonicity; 2, wobbly gait; 3, complete hind limb paralysis; 4, complete hind and fore limb paralysis; 5, moribund or dead. The central nerve system tissues from EAE mice were then isolated and analyzed as previously described (Wang et al., 2012).

Cytospin and immunofluorescence staining

Naive T cells were polarized under Th17 culture condition for 24 h and then re-suspended in culture medium at 1 million/mL. ~100 μL of each cell suspensions were added to a slide chamber, and spun down onto the slide using a cytocentrifuge (800 rpm/5 min). The cells were fixed on slide with 4% PFA, permeabilized with 0.01% TrionX-100, blocked with goat serum and stained with αSMAD4 antibody (Santa Cruz, Cat# sc-7966) overnight. The slides were washed and then incubated with goat anti-mouse IgG (Biolegend, Cat# 405319) or APC conjugated goat anti-mouse IgG (Biolegend, Cat# 405308) secondary antibody for 2 h at room temperature, and finally mounted with mounting medium containing DAPI. The images were obtained by LSM780 fluorescence microscope (Zeiss). The translocation ratio was measured using Image-Pro Plus 6.0 software and calculated based on the relative intensity of SMAD4 staining in the nucleus or cytoplasm.

SUMOylation assay

Total $CD4^+$ T cells, enriched by the MACS mouse $CD4^+$ T cell isolation kit (Miltenyi), were cultured under Th17 polarizing condition at 37°C or 39.5°C for 24 h, and then harvested and lysed by 1% SDS containing 20 mM NEM to preserve SUMOylation. The cell lysates (containing 50 mM DTT) were denatured at boiling temperature for 10 min followed by sonication to reduce viscosity. After 10-fold dilution using RIPA buffer, the immunoprecipitation was performed using αSMAD4 (Abcam, Cat# ab40759) and Dynabeads Protein A (Life Technologies, Cat# 10002D) to enrich the targeted protein, and SUMOylated bands were detected by western blotting with αSUMO2 antibody (Invitrogen, Cat#519100).

ChIP-seq

The ChIP assay was performed using Active Motif's ChIP assay kit (53035) according to manufacturer's instructions with slight modifications (Jiang et al., 2018). Briefly, Th17 cells were harvested and then cross-linked with 1% paraformaldehyde for 10 min and stopped with 125 mM glycine for 5 min at room temperature. The cells were lysed and digested with shearing enzyme followed

by 10 cycles' sonication. The cell lysate was then used for immunoprecipitation with antibodies αSMAD4 (Abcam, Cat# ab40759) or control IgG (Abcam, Cat# ab46540) followed by Dynabeads Protein A (Life Technologies, Cat# 10002D) pulldown. The precipitated DNA was then washed, eluted, de-crosslinked and purified for realtime PCR analysis or for deep sequencing carried by BGI Genomics. The sequence data were deposited in the GEO database under the accession number: GenBank: GSE125263. The primers used for ChIP-QPCR are listed in supplementary table.

Clean reads after filtering were aligned to the reference sequence mm10 genome by using bowtie2 (Langmead and Salzberg, 2012). PCR duplicates were removed using picard MarkDuplicates. The uniquely mapped reads were used to call peak with MACS2 (Zhang et al., 2008) using a p value cutoff 0.01. ChIPseeker was used for peak annotation (Yu et al., 2015). Deeptools was used to generate coverage track file (bigWig) which can be visualized in IGV

RNA-seq

Th17 cells were collected after 3 days culture and the total RNA was extracted with Trizol (Life Technologies) according to manufacturer's instructions, and the RNA-seq library was constructed and sequenced with BGI500 platform by BGI Genomics. Low quality reads and adaptor sequences were removed by Trim Galore v0.4.4. The clean reads were mapped to the *Mus musculus* genome (version mm10) by bowtie2 with default parameter. The unique mapping reads were summarized by featureCounts (from Subread package). Differentially expressed genes were identified by at least 1.5 fold change and FDR adjusted p value 0.01 (Wang et al., 2010). The pathway analysis was performed with ClusterProfiler (R package) (Yu et al., 2012). The sequence data were deposited in the GEO database under the accession number: GenBank: GSE125264.

For comparison, febrile temperature induced genes were compared with previously reported pathogenic Th17 cells induced by TGF-β3 (GenBank: GSE39820), or generated in the EAE model versus homeostatic state, by overlay or GSEA. The pathogenic and non-pathogenic gene-sets used for comparison was determined by differential expressed genes between TGF-β3 versus TGF-β1 induced Th17 cells, or Th17 cells induced with IL-23 versus without IL-23 (GenBank: GSE23505), or Th17 cells induced in the EAE model versus homeostatic state.

Real-time PCR

T cells derived from the adoptive T cell transfer models will be sorted based on $CD4^+CD3^+$ surface markers and used for mRNA preparation. T cells collected in *in vitro* cultures will be first restimulated with plate bound αCD3 for 4 h to stimulate cytokine gene expressions before harvesting. The total RNA from these cells was extracted by TRIzol (Invitrogen) according to manufacturer's instruction. The cDNA was synthesized by reverse transcription using M-MLV Reverse Transcriptase (Promega) according to the manufacturer's instructions and used for realtime PCR assay, performed in 1x Hieff qPCR SYBR Green Master Mix (Yeasen) together with 0.2 μM forward and reverse primers. The mRNA amounts of indicated genes were normalized against that of β-Actin, and the ChIP-QPCR data were normalized to input.

QUANTIFICATION AND STATISTICAL ANALYSIS

All our *in vitro* and *in vivo* data were repeated at least 2-5 times with consistent results. When indicated, the statistical significance was shown as mean ± SD and generally determined by Student's t test, or Two-way Anova analysis when indicated. (* represents $p < 0.05$; ** represents $p < 0.01$; *** represents $p < 0.001$).

DATA AND CODE AVAILABILITY

The accession number for RNA-seq data reported in this paper is GenBank: GSE125264. The accession number for ChIP-seq data reported in this paper is GenBank: GSE125263.